Rijkswaterstaat
Ministerie van Infrastructuur en Milieu

NL-LAB

Nederlands programma voor Langjarige Asfalt Bemonstering

Seleridis Georgios

November 2016

Department of Civil Engineering and Geosciences

Delft University of Technology

Rijkswaterstaat

A technical report presented as the product of the internship carried out at Rijkswaterstaat

---

NL-LAB

Author:

Georgios Seleridis

Supervisors:

Prof. S. Erkens

Dr. R. Hofman

PREFACE

This report was written during my time at the GPO department of Rijkswaterstaat in The Netherlands, as part of an internship during my Master in Structural Engineering at TU Delft. The internship took place from the 1st of September 2016 and lasted for 12 weeks, until 30th of November. My main task was within an on-going project of Rijkswaterstaat, named NL-LAB.

This report contains all the literature review required as background knowledge for this project, along with the analysis and calculations performed based on them. Several conclusions and recommendations for future implementation on the project are the outcome of my research.

I want to express my gratitude to Prof. Sandra Erkens, my supervisor at TU Delft, for the time she spent and the interest she showed in my progress. I also want to thank Mr. Jan Voskuilen and Mrs. Inge van Vilsteren from Rijkswaterstaat for guiding and trusting me with responsibilities through the project.

TABLE OF CONTENTS

1. INTRODUCTION 4

1.1 NL-LAB Project 4

1.1.1 Initiation 4

1.1.2 Aim 5

1.1.3 Research Questions 5

1.1.4 Overall Approach 5

1.1.5 Materials 7

1.2 Recipe Based and Functional Characterization of Asphalt Mixtures 8

1.3 Previous research at TU Delft 9

1.3.1 Permanent deformation 9

1.3.2 Water Sensitivity 10

1.4 Subject and duties of this internship within NL-LAB 10

1.5 Relevance and Importance for Rijkswaterstaat 10

1.6 Relevance and Importance for Contractors 11

2. MOISTURE SENSITIVITY 12

2.1 Literature Review 12

2.1.1 Definition 12

2.1.2 Adhesion 13

2.1.3 Cohesion 13

2.1.4 Influencing factors 14

2.1.5 Brief test description 15

2.2 Water Sensitivity prediction 16

2.2.1 Regression analysis principles 16

2.2.2 MEPDG methodology 17

2.2.3 NEN standard 18

2.2.4 Correspondence of MEPDG and NEN 19

2.2.5 Analysis and results 20

2.3 Comparison of Lab to Field measured properties 24

2.3.1 Data analysis 24

2.3.2 Explanatory factors 27

2.3.3 Conclusion 30

3. PERMANENT DEFORMATION 32
3.1 Literature Review 32
3.1.1 Definition 32
3.1.2 Types of rutting 32
3.1.3 Development stages 34
3.1.4 Influencing factors 35
3.1.5 Brief test description 37
3.2 Permanent deformation prediction 38
3.2.1 MEPDG Methodology 38
3.2.2 NEN standard 40
3.2.3 Correspondence of MEPDG and NEN 42
3.2.4 Analysis and results 44
3.3 Comparison of Lab to Field measured properties 52
3.3.1 Data analysis 52
3.3.2 Explanatory factors 55
4. CONCLUSION 59
4.1 Research Conclusion 59
4.1.1 Water sensitivity prediction 59
4.1.2 Water sensitivity lab and field comparison 59
4.1.3 Permanent deformation prediction 60
4.1.4 Permanent deformation lab and field comparison 61
4.2 Recommendations for further research 61
5. REFERENCES 64

1. INTRODUCTION

1.1 NL-LAB Project

The project that was the main subject of this internship is called "NL-LAB" and stands for National-Living Lab. This programme started in 2012, and is the successor of Rijkswaterstaat's "FEC" programme (Functionele Eisen in het Contract) in the period of 1999 – 2005. It is conducted by Infraquest which is a collaboration of three parties; Rijkswaterstaat, TU Delft and TNO.

1.1.1 Initiation

In 2008, the harmonized CEN standards for Asphalt Concrete were introduced in Europe. The way to characterize several types of Asphalt mixtures, Reclaimed Asphalt and the requirements for testing the mixes, and ensuring production quality are described in a series of standards. For Asphalt Concrete (13108-1) the standard offers the choice between a classical, recipe based characterisation or a functional characterisation, based on more mechanical-type properties in combination with some limited composition requirements.

Between these two methods of characterization, the Netherlands adopted the functional characterisation for AC mixtures, with the aim of developing a more fundamental and in-depth understanding of asphalt concrete response, providing in this way the opportunity to develop well performing mixtures. However, the current understanding at that point was far from complete, despite the fact that the experiences since 2008 showed that, this approach allows for a better, more fundamental understanding of Asphalt Concrete. Especially the effect of higher percentages (60-70%) of reclaimed asphalt led to surprising observations, since it appeared to improve all functional requirements, without the typical interrelation where an increase in stiffness corresponds with a decrease in fatigue resistance. These experiences led to the initiation of this program using the Dutch road network as a living laboratory [1].

1.1.2 Aim

For some, especially low temperature mixtures, laboratory production proved difficult. This raised the question of how well actual field conditions are represented by lab conditions, which has a direct impact on the reliability of the performance predictions. These questions along with the experiences mentioned previously, led to this long term research program, through long term field monitoring. Its aim is:

1. To get an up to date reference frame based on commonly used mixtures, as well as a frame work for the evaluation and possibly improvement of the functional tests and the requirements based on them.
2. Assess the effects of mixing and compaction on functional properties, in combination with actual laboratory research on mixes used in pavement construction projects.
3. Establish the predictive quality of lab determined functional properties for field performance [1].

1.1.3 Research Questions

The research questions that were derived through the experiences and developments that initiated the program are:

1. How (well) do the functional characteristics relate to field performance?
2. Is testing on laboratory mixed and compacted the correct choice?
3. Are the current tests able to distinguish “good” from “bad” mixtures?
4. How accurate and reliable can the prediction of a mixture’s performance be, based on its volumetrics?

1.1.4 Overall Approach

As mentioned, the Dutch road network is used as a living laboratory to answer the research questions. Although the Netherlands is a small country, the density of its road network (6^{th} densest of the world with 331km of road per $100km^2$ of land area), provide ample opportunity for field testing.

However, field tests alone will not provide answers to the research questions. The program combines lab testing with field monitoring as follows:

I. Assess the effect of mixing and compaction on the lab determined properties.

This step is addressed by making specimens in three different ways:

- *Phase 1 (F1):* Lab Mixed – Lab Compacted
- *Phase 2 (F2):* Plant Mixed – Lab Compacted
- *Phase 3 (F3):* Plant Mixed – Field Compacted (specimens taken from the pavement)

This step gives insight in the effects of mixing and compacting as well as providing a first indication of the relation between the predictive quality of lab mixed and compacted for field properties.

II. Follow the changes of lab determined properties over time.

Directly after construction, specimens were taken for immediate testing (F3), as well as for testing after 2 (F4) and 6 years (F5). These plates are stored under controlled conditions. This way the effect of traffic is excluded and the changes in properties are solely related to changing material characteristics, related to ageing.

III. Monitor the pavement performance over time.

This is straight forward for wearing courses, whereas for binder and base courses it is more complicated. For those locations the monitoring is more indirect, based on the performance of the pavement structure as a whole.

IV. Predict the functional properties.

By making use of the data already recorded for the previous steps, the predictive quality of lab determined functional properties for field performance is established. For the purposes of this internship this was done based on the Mechanistic – Empirical Pavement Design Guide (MEPDG) formed by the National Cooperative Highway Research Program (NCHRP) in the USA.

1.1.5 Materials

The program consists of 4 works, each referring to a different batch of specimens provided by different contractors. Each batch has different mixture design characteristics (seen in the table below), to assess the effect of their variation on the performance of AC. Works 1 and 2 were distributed in two different labs to assess the effect of different construction and test conditions. Work 5 is scheduled to be added in 2017. The passing material percentages in the final mix composition might slightly differ from the design values due to measuring accuracy limitations in their construction.

Table 1. Characteristics of mixtures tested

Construction Project	A4		N345		A28, HRL 157.700-156.100km		Bennenbroekerweg te Hoofdorp	
Contractor	OOMS/MNO		KWS		Van Der Lee		Boskalis	
Mix Identification	P1		P2		P3		P4	
Mixture Type (EN13108-1)	AC 22 Base		AC 22 Base 35/50, 60% PR		AC 22 Base/Bind		AC 22 base 40/60 60% PR	
Mixture Code	251		167163/267163		27774		A252	
Date Type Test Report	23-11-2011		09-09-2011		11-2013		21-12-2011	
Report Number Type Test	K FEC 2.0 APRR Platen		035-11		FEC 2.0_fase A		11806364 A	
Constituent Materials	% "IN" 100% mass							
Stone	Norwegian Granite 8/16	7,2	Bestone 8/11	14,92	Scottish Granite 16/22	10,8	Scottish Granite 16/22	8
	Norwegian Granite 16/22	9,6	Bestone 16/22	8,93			Scottish Granite 8/16	13,8
	ECO-gravel	10,0						
Sand	ECO-sand	20,3	Course sand	13,17	River sand	20	Washed sand	12
Filler	Baghouse dust	1,0	Own Dust	1,22	Wigras 40k	2,6		
Reclaimed Asphalt	Crushed DAC 0/20	25,0	Crushed DAC 0/20	57,36	Milled AC 0/16	32,5	Frees 0/20	32,5
	Milled PA	25,0			Milled PA 0/16	32,5	Gebroken frees 0/20	32,5
Bitumen	70/100	1,9	70/100	1,76	160/220	1,6	70/100	1,6
	From RAC	2,4	From RAC	2,6	From RAC	2,4	From RAC	3,1
Composition	% Through Sieve							
C22.4	100,0		100,0		99,0		97,0	
C16	94,9		91,0		87,0		90,0	
C11.2	80,5		84,0		80,0		80,0	
C8	64,9		71,0		60,0		65,0	
C5.6	55,0		58,0		52,0		55,0	
2 mm	39,9		47,0		43,0		44,0	
63 µm	5,6		6,9		8,0		6,6	
Filler	5,6		6,6		8,0		6,6	
Bitumen (in 100% mass)	4,3		4,3		4,5		4,3	

1.2 Recipe Based and Functional Characterization of Asphalt Mixtures

The main reason that triggered the initiation of NL-LAB was the transition from the traditional recipe based characterization to the functional characterization. A characteristic of a recipe based (empirical) method is that it relies on practical experience rather than theories. This makes an empirical method descriptive rather than explaining. An empirical law can describe a phenomenon without providing an understanding, although the empirical law itself could be considered a sort of "understanding"; yet, this differs from an understanding in terms of fundamental principles, which have more general predictive value. An empirical law is predictive merely in its own reference system.

A system of contractual requirements and technical specifications works satisfactorily as long as it is operated within its framework of standardised technology. With any new development the road authority asks if current requirements are applicable, and if not, to develop new requirements. This question unfolds the recipe-based system's restriction. The restriction lies in its empirical character. This causes the limited applicability of the current requirements and specifications to newly developed products, and the long time needed to evaluate the performance of new products, and, because of that, also a long time to develop new requirements. The time needed to develop new requirements, let alone the time needed to develop the knowledge to be able to develop a more fundamental approach, causes the implementation of innovative techniques and materials to stay at a low pace, until a system is developed which permits development of more generally applicable requirements.

An empirical methodology requires renewal of empirical reference data, based on practical experience. To gain practical experience with a new pavement design, or a new type of asphalt mixture, requires monitoring of the nominal service-life, to gather reference data, and to verify the performance (cost-effectiveness with respect to standard pavement designs, respectively asphalt mixtures). This leads to a delay of innovation that was no longer acceptable. To improve this situation, it seems that requirements have to be more generally applicable, not just to standardised technology but to new technology as well. In a functional or performance related approach concerned with the prediction of pavement behaviour, and the evaluation of the cost-effectiveness and risk of failure, the material composition is irrelevant; relevant are only the properties needed to predict or judge the cost-effectiveness and the risk of failure [2].

In particular, Dutch standards set requirements for four functional characteristics of AC:

1. **Resistance to Fatigue**

   EN 12697-2: Four point bending in continuous, full sinusoidal strain control at 20°C and 30Hz, aimed at determining the strain at which the material can take $1x10^6$ load repetitions.

2. **Stiffness**

   EN 12697-26: Four point bending in continuous, full sinusoidal strain control at 20°C and 8Hz.

3. **Water Sensitivity**

   EN 12697-12: ITS ratio determined by the conditioned and unconditioned ITT of the material at 15°C.

4. **Resistance to Permanent Deformation**

   EN 12697-25: Cyclic triaxial compression, temperature and loading conditions dependent on the position of the material in the pavement, aimed at determining the minimum slope of the permanent deformation versus load repetition curve.

Within NL-LAB, contractors performed the tests on the AC samples they provided, whereas the bitumen tests were performed by TNO.

In addition to the type-tests results provided in the contractor's report, all the necessary mixture characteristics are also recorded as part of the contract. These include:

- Specimen Code
- Date of production
- Thickness and diameter
- Mass
- Mass submerged
- Mass wet
- Temperature of water
- Density
- Percentage of air voids

1.3 Previous research at TU Delft

1.3.1 Permanent deformation

In 2013 a research was done on behalf of NL-LAB by Mr. Berti Carlo, exchange Master student at TU Delft, as part of his final thesis. The thesis focused on the permanent deformation resistance prediction. At that point the available data included work 1 and 2. His research was used as a preliminary indication for this internship's research.

1.3.2 Water Sensitivity

Along with Mr. Berti, Mr. Florio Eugenio, also exchange Master student at TU Delft, conducted a research within NL-LAB. His thesis focused on the water sensitivity resistance prediction, also using the data from works 1 and 2. Both students carried out their research also aiming to compare the European and American mix design approaches, thus the MEPDG was used as their basis.

1.4 Subject and duties of this internship within NL-LAB

By August 2016, just before the start of the internship, contractors had carried out the type-tests up to Work 4 for phases 1-2-3-4, meaning that a large amount of additional data was available. Rijkswaterstaat at that point had completed the interpretation and analysis of the results up to Work 1, not including the permanent deformation tests. Mr. Berti and Mr. Florio had carried out the permanent deformation and water sensitivity analyses respectively, but they were not officially included in NL-LAB's report at that time. Works 2, 3 and 4 were pending.

After discussions with the parties involved, the emphasis of this internship was decided to be on two of the four functional properties included in NL-LAB, Permanent Deformation and Water Sensitivity, taking into consideration all 4 works available. The analysis is divided in two main parts for each property:

1) Derivation of a performance prediction formula via a regression analysis
2) Comparison of the lab and field determined properties (F1 vs F3)

1.5 Relevance and Importance for Rijkswaterstaat

- Assess the reliability and effectiveness of a contractor's work based on the comparison between the lab and field results they provide.
- Establish more deeply understood requirements related to functional characterisation of asphalt concrete.
- Modify the regulations and test procedures due to the redefined distinction between "good" and "bad" mixtures and tests.

- Conclude as to whether recycled asphalt leads to better asphalt performance thus changing its policy to a more recycling-oriented direction.
- Endorse competition in the research field regarding the introduction of innovations in asphalt mixtures, by abolishing the restrictions necessitated by the recipe based design.

1.6 Relevance and Importance for Contractors

- Save time and money by avoiding the time-consuming and expensive lab tests. The calculation of asphalt performance is done by using the relations provided by RWS instead of carrying out the type-tests. This will give them a good indication of the properties in the preliminary design phase of the mixture.
- Freedom for the introduction of innovations and new materials. Restrictions resulting from recipe-based mixtures no longer apply.
- A new wide space of economic benefit potential for the contractors themselves, and by extension, benefit for the final user of the product, in this case the public.

2. MOISTURE SENSITIVITY

2.1 Literature Review

2.1.1 Definition

One of the main factors that affect a bituminous mixture's durability is moisture damage, along with age hardening. Ageing of the binder results in a stiffness (or viscosity) increase. Moisture damage is mostly manifested through three mechanisms: (1) loss of cohesion through a gross softening of the bitumen or weakening of asphalt concrete mixtures, (2) loss of adhesion between the aggregate and the bitumen, also known as stripping, and (3) degradation or fracture of individual aggregate particles when subjected to freezing. It is a generally agreed fact that moisture has a disrupting effect in the integrity of the structure of bituminous mixtures, through these three mechanisms.

Reduction of the strength and stiffness of a mixture is often the result of cohesion reduction. A pavement with reduced strength loses its ability to support traffic-induced stresses and strains. Also, loss of bond between aggregate and bitumen, leads to a reduction in pavement support as well. Both mechanisms result in weaker pavement layers which are susceptible to deformations under traffic loading, and in the case of stripping, loss of material and deterioration of the mixture.

Picture 1. Fatigue cracking caused by stripping [3]

2.1.2 Adhesion

An understanding of the factors that cause the loss of adhesion requires the knowledge of the mechanisms through which it occurs in a mixture. There are 4 main ways of asphalt binder – aggregate adhesion:

- Mechanical

  Irregularities and pores in the surface of the aggregate allow the asphalt binder to enter and create an interlock with its hardening. In case moisture is present on the aggregate, it can interfere with the binder's penetration in the aggregate and deteriorate the mechanical interlock. This increases the susceptibility to stripping.
- Chemical

  Chemical adhesion is caused through the asphalt binder's and aggregate's surface chemical reaction. Generally, aggregates with acidic surfaces react weaker with asphalt binders, potentially resulting to other moisture damage factors, if not sufficiently strong.
- Adhesion tension

  "Wetting line" is the edge of the drop, as a drop spreads over a surface. The tension between the asphalt binder and aggregate along the wetting line is in general lower than the tension between water and aggregate. For this reason, if all three are in contact, asphalt binder will be displaced by water, resulting in poor wetting of the aggregate surface by the asphalt binder. This is a cause of stripping.
- Molecular orientation

  When in contact with aggregate, asphalt molecules tend to orient themselves in relation to the ions on the aggregate surface essentially creating a weak attraction between the asphalt binder and aggregate surface. If water molecules, which are dipolar, are more polar than asphalt binder molecules, they may preferentially satisfy the energy demands of the aggregate surface. The resulting weak asphalt binder-aggregate bond can result in stripping [3].

It is most likely that two or more mechanisms occur simultaneously in a mixture to cause loss of adhesion, and all of them may occur to some extent in any asphalt- aggregate system.

2.1.3 Cohesion

Under the assumption that adhesion between aggregate and asphalt is adequate, cohesive forces will develop in the asphalt film or matrix. Factors such as viscosity of the asphalt-filler system can influence the cohesion values. Water can affect cohesion though the intrusion into the asphalt binder film or through saturation and expansion of the void system (swelling) [4].

2.1.4 Influencing factors

Moisture susceptibility is a phenomenon which depends upon the mechanisms described above, hence its complexity. Their interaction makes it difficult to predict with certainty the importance of a particular characteristic as a factor in determining moisture susceptibility. A general rule suggests that «moisture susceptibility is increased by any factor that increases moisture content in the HMA, decreases the adhesion of asphalt binder to the aggregate surface or physically scours the asphalt binder» [3]. The factors described below have an influence on moisture susceptibility, but none of them as fully definitive for predicting it. They refer to the mixture design and construction characteristics, but not climatic or traffic conditions.

- Asphalt binder characteristics
  Viscosity is an important property of bitumen because it may be an indicator of higher asphaltenes concentrations, which can create higher adhesion tension and molecular orientation adhesion. For this reason, lower viscosities, and consequently lower asphaltenes concentrations, are in general more susceptible to stripping. Other components in asphalt binders such as sulfoxides, carboxylic acids, phenols and nitrogen bases can also potentially lead to stripping.
- Aggregate characteristics
  Hydrophilic aggregates (attract water) are more prone to strip than hydrophobic aggregates (repulse water). The key properties that determine this characteristic are the surface chemistry (acidic aggregate surfaces are more susceptible to stripping), porosity and pore size; high porosity leads to high absorption and more asphalt binder has to be used to achieve the desired effective binder content. If this is not considered, not sufficient binder will be available for the creation of the film around aggregate particles, resulting in faster aging and stripping.
- Air voids
  When air voids exceed about 8% of the volume, they will possibly become interconnected and allow water to penetrate with ease, causing moisture damage through pore pressure or ice expansion. For this reason, mix design has to adjust binder content and aggregate gradation, to achieve the desirable void content. Construction stage also defines this factor. Inadequate compaction will result in lower density levels, meaning that more voids than the

designed remain in the mixture's structure. Poor compaction can be caused either by not well executed compaction plan, or by cool weather condition during the construction.

2.1.5 Brief test description

Typically, for the evaluation of the severity of moisture damage, the test consists of a conditioning phase and an evaluating phase. The conditioning phase simulates the field pavement conditions that increase water sensitivity. The evaluation phase measures the strength for the estimation of the severity of moisture damages, by the calculation of a strength ratio. Usually one specimen is conditioned, another one is unconditioned, and afterwards the ratio between the conditioned and unconditioned strength is computed. If the ratio is less than a specified value, the mixture is characterized as moisture susceptible.

There is a variety of methods that can be used to evaluate moisture sensitivity. The method used for this project is described by the European Standards in EN 12697-12 and follows the principle below:

"A set of cylindrical test specimens is divided into two equally sized subsets and conditioned. One subset is maintained dry at room temperature while the other subset is saturated and stored in water at elevated conditioning temperature. After conditioning, the indirect tensile strength (ITS) of each of the two subsets is determined in accordance with EN 12697-23 at the specified test temperature. The ratio of the indirect tensile strength (ITSR) of the water conditioned subset compared to that of the dry subset is determined and expressed in percent."

The tests were performed at the temperature of 15 ^{o}C in accordance to the standard specifications, while the conditioning took place at 40 ^{o}C, for a period of about 70 hours. The specimens dimensions for all works were 50 mm in thickness and 150 mm in diameter, with minor deviations in the range of 0,1 mm caused during their extraction. In total 49 samples from 4 works were tested, plus 10 aged samples from the field specimens after the passing of 2 years, making up the total of 59 ITS measurements. Prior to the tests all their volumetric properties were recorded.

2.2 Water Sensitivity prediction

2.2.1 Regression analysis principles

When the subject of a research is, based on a specific dataset available, to come up with a relation that describes a property, the mathematical tool used to achieve this is regression analysis. Regression analysis is a statistical process for estimating the relationships among variables. It includes many techniques for modelling and analyzing several variables, when the focus is on the relationship between a dependent variable and one or more independent variables. More specifically, regression analysis helps one understand how the typical value of the dependent variable (the mixture's functional performance) changes when any one of the independent variables is varied (the mixture's design characteristics). In our case, an extension of the simple linear regression is used, the multiple regression analysis. It is used when we want to predict the value of a variable based on the value of two or more other variables.

Having a big amount of data available from the tests, like mixtures' volumetrics and bitumen's characteristics (independent variables), the multiple regression will give the desired predictive relation. It is a common case for an independent variable to lead to a good prediction of a dependent one, due to purely statistical reasons, without any explained physical relation. For this reason during this process, the decision of which variables are the most suitable to use in terms of engineering connection with the performance of the mixture, is critical for the quality of the prediction.

The quality of the prediction relation and how well it fits in the measured data is determined by the coefficient of determination, denoted as R^2 or R-squared, which is a number that indicates the proportion of the variance in the dependent variable that is predictable from the independent variable. An ideal fit would give and R^2 value of 1. However, in engineering a good and acceptable fit is considered for R^2 values above 0,75. The calculation of R-squared is done as follows:

$$SS_E = \sum_i \left(y_i - \hat{y}_i\right)^2$$

$$SS_T = \sum_i \left(y_i - \overline{y}_i\right)^2$$

$$R^2 = 1 - \frac{SS_E}{SS_T}$$

where,

SS_E = explained sum of squares

SS_T = residual sum of squares

y_i = measured values of the dependent variable

$\hat{y}_i$ = calculated values of the dependent variable

$\overline{y}_i$ = mean value of the measured values of the dependent variable

The computational tool, used to perform the regression analysis, was initially the built-in regression function of Microsoft Excel. A custom manual regression set of calculations was then developed using Excel's solver. In a comparison between the two tools, the custom made tool gave slightly better quality fits, hence a combination of both tools was used for the remaining analyses.

Based on an initial set of multipliers, the calculated values of the dependent variable are obtained. Then the R-squared value of this calculation is computed. What solver is used for is to minimize the explained sum of squares SS_E, and consequently maximize R-squared, through a big number of iterations in the multipliers values. The iteration stops when no further improvement can be achieved. However, since the solver function heavily depends on the initial values of the iterations, giving values which are totally out of range of the optimum, causes the function to fail and give no result. For this reason, the automatic regression of Excel was used to obtain an indicative set of initial multipliers, and then solver optimized these sets.

2.2.2 MEPDG methodology

The starting point for this analysis, as used by Mr. Florio in his research as well, was the NCHRP Design Guide 1-37A which describes a uniform and complete set of procedures for the design of rehabilitated and new flexible and rigid pavements. This methodology, often termed as Mechanistic-Empirical Pavement Design Guide (MEPDG), specifies a formula aimed at predicting the Indirect Tensile Strength of a given mixture. This ITS formula is reported below:

$$ITS = 7416,712 - 114,016 \cdot V_a - 0,304 \cdot V_a^2 - 122,592 \cdot VFA + 0,704 \cdot VFA^2 + 405,71 \cdot \log(Pen_{77}) - 2039,296 \cdot \log(A)$$

where,

ITS = Indirect Tensile Strength at -10°C (psi)

Va = Air Void content (%)

VFA = Voids Filled with Asphalt (%)

Pen_{77} = Binder penetration at 77°F (or 25°C) (mm/10)

A = Viscosity-Temperature susceptibility intercept

The intercept of binder viscosity – temperature relationship is calculated as follows:

$$A = \frac{\log Pen_{77} - \log 800}{25 - T_{R\&B}}$$

where,

Pen_{77} = Pen_{25} = penetration of bitumen at 77°F (or 25°C)

$T_{R\&B}$ = softening point of bitumen (°F or °C)

The Design Guide procedures to establish this formula followed the Indirect Tensile Test performed at a temperature of -10°C using a loading rate of 51 mm per minute, eventually reporting the strength in psi. As described previously, the specimens within NL-LAB were tested at 15°C, at a loading rate which complied with the European standards, reporting the strength values in kPa. This implies that a series of recalculations and elaborations needed to be made in order to calibrate this formula and make it applicable to the European conditions. New sets of parameter multipliers have to be obtained for this purpose.

2.2.3 NEN standard

The test procedures regarding water sensitivity, as defined by the European standards, are described in "NEN-EN 12697-12: Bituminous mixtures – Test methods for hot mix asphalt – Part 12: Determination of the water sensitivity of bituminous specimens". The method followed is described in a previous chapter. According to this method, the moisture sensitivity of a bituminous mixture is described by the Indirect Tensile Strength Ratio, ITSR:

$$ITSR = 100 \times \frac{ITS_{wet}}{ITS_{dry}}$$

where,

ITSR = the Indirect Tensile Strength Ration (%)

ITS_{wet} = the average indirect tensile strength of the wet group (kPa)

ITS_{dry} = the average indirect tensile strength of the dry group (kPa)

2.2.4 Correspondence of MEPDG and NEN

Due to the fact that the Design Guide's relation refers to the indirect tensile strength and the European standard refers to the ratio, the comparison cannot be made directly. In this research, two different ways of setting the target for the regression analysis were followed, giving three R-square values for the prediction quality:

1. Predicting dry and wet specimens' indirect tensile strength as two separate tests, with no interference between them.

$$ITS_{calculated,dry} = \alpha_o + \alpha_1 \cdot V_a + \alpha_2 \cdot V_a^2 + \alpha_3 \cdot VFA + \alpha_4 \cdot VFA^2 + \alpha_5 \cdot \log(Pen) + \alpha_6 \cdot \log(A)$$

$$ITS_{calculated,wet} = \beta_o + \beta_1 \cdot V_a + \beta_2 \cdot V_a^2 + \beta_3 \cdot VFA + \beta_4 \cdot VFA^2 + \beta_5 \cdot \log(Pen) + \beta_6 \cdot \log(A)$$

In this way, two independent set of parameters are calculated, α_i and β_i, based on the separate R-square values of dry and wet ITS prediction formulas.

2. Predicting the ratio between wet and dry indirect tensile strength.

$$ITS_{calculated,dry} = \alpha_o + \alpha_1 \cdot V_a + \alpha_2 \cdot V_a^2 + \alpha_3 \cdot VFA + \alpha_4 \cdot VFA^2 + \alpha_5 \cdot \log(Pen) + \alpha_6 \cdot \log(A)$$

$$ITS_{calculated,wet} = \beta_o + \beta_1 \cdot V_a + \beta_2 \cdot V_a^2 + \beta_3 \cdot VFA + \beta_4 \cdot VFA^2 + \beta_5 \cdot \log(Pen) + \beta_6 \cdot \log(A)$$

The individual ITS values are calculated using the same type of formula. Then the ITSR is back-calculated as follows:

$$ITSR_{calculated} = 100 \times \frac{ITS_{calculated,wet}}{ITS_{calculated,dry}}$$

The difference lies in the fact that the change in the parameters of the ITS terms is done with the aim of maximizing the ratio's prediction accuracy. The R-square in this case refers to the quality of the ITSR prediction, which is done by finding the optimum combination of α_i and β_i that leads to the closest to reality value of ITSR.

2.2.5 Analysis and results

The initial parameters taken into account are the ones seen in the previous paragraph. The principle followed after that was to gradually add extra parameters, change their format, or exclude them in different possible combinations. This was done for both regression targets mentioned above; one aiming at maximizing the individual R-squares of dry and wet (top row of R^2 at tables 2 and 3), and one aiming at maximizing their ratio's R-square (bottom row of R^2).

In total, 59 data points were taken into consideration, including works 1, 2, 3 and 4. In the case of work 3 though, *G** values were not provided by the contractor, thus in the sets that it was included as a parameter, work 3 was completely excluded. The concept behind parameter sets combination and their contribution to the quality of the fit is discussed below:

Set 1	Initial parameters suggested by MEPDG.
Set 2	Density is added due to its explained connection to moisture susceptibility
Set 3	Squared terms of V_a and *VFA* are excluded because of their unexplained physical contribution to the regression and the redundancy if included in both forms
Set 4	Squared terms of V_a and *VFA* included instead of the non-squared, for the redundancy reason explained in set 3
Set 5	Bitumen content added to set 2 because so far it was the best in terms of R^2. Bitumen content is related to the film thickness in the aggregates surface
Set 6	Viscosity-temperature intercept excluded
Set 7	$T_{R\&B}$ added. As explained, from the bitumen properties, only two shall be used at the same time, in this case *Pen* and $T_{R\&B}$
Set 8	Bitumen stiffness *G** at 0,1 rad/s added. From this point on, work 3 is not taken into account
Set 9	Exclusion of V_a and *VFA* squared for the reasons mentioned in set 3, this time including *G**
Set 10	Same parameters with set 2 plus the addition of *G** to see how all terms work together
Set 11	Further addition of bitumen content to set 10
Set 12	Replacement of Pen with $T_{R\&B}$
Set 13	Removal of squared terms from set 11
Set 14	Removal of logarithm from *Pen* term
Set 15	The parameters used are identical to set 7. The difference lies in the data points used. Set 7 uses all the works available, whereas set 15 excludes work 3, even though it is available.

	This is done to assess whether the increase from set 7 to 8 in R^2 with the addition of *G** occurs due to its contribution to the quality or due to the fact that work 3 is excluded because it is missing
Set 16	Air void content completely excluded. *Pen* is used without logarithm
Set 17	Voids filled with asphalt excluded as well
Set 18	Only volumetric properties included
Set 19	Only bitumen properties included

Table 2. Parameter Sets (1/2)

Set		1	2	3	4	5	6	7	8	9	10
		Intercept	Intercept	Intercept	Intercept	Intercept	Intercept	Intercept	Intercept	Intercept	Intercept
		V_a	V_a	V_a	-	V_a	V_a	V_a	V_a	V_a	V_a
		V_a^2	V_a^2	-	V_a^2	V_a^2	V_a^2	V_a^2	V_a^2	-	V_a^2
		VFA	VFA	VFA	-	VFA	VFA	VFA	VFA	VFA	VFA
		VFA^2	VFA^2	-	VFA^2	VFA^2	VFA^2	VFA^2	VFA^2	-	VFA^2
		logPen	logPen	logPen	logPen	logPen	logPen	logPen	logPen	Pen	logPen
		logA	logA	logA	logA	logA	-	-	-	-	logA
		-	Density	Density	Density	Density	Density	Density	Density	Density	Density
		-	-	-	-	V_{bit}	V_{bit}	V_{bit}	-	-	-
		-	-	-	-	-	-	$T_{R\&B}$	-	-	-
		-	-	-	-	-	-	-	G*	G*	G*
R^2	**ITS $_{dry}$**	0,46	0,46	0,43	0,44	0,47	0,23	0,47	0,50	0,42	0,54
	ITS $_{wet}$	0,30	0,38	0,29	0,29	0,39	0,29	0,38	0,54	0,46	0,60
	ITSR	0,09	0,41	0,28	0,28	0,39	0,34	0,40	0,64	0,60	0,67
R^2	ITS $_{dry}$	0,41	0,40	0,40	0,44	0,42	0,16	0,41	0,44	0,38	0,50
	ITS $_{wet}$	0,21	0,36	0,29	0,27	0,33	0,25	0,35	0,54	0,46	0,60
	ITSR	0,28	0,52	0,34	0,35	0,51	0,47	0,54	0,70	0,65	0,71

Table 3. Parameter Sets (2/2)

Set		11	12	13	14	15	16	17	18	19
		Intercept	Intercept	Intercept	Intercept	Intercept	Intercept	Intercept	Intercept	Intercept
		V_a	V_a	V_a	V_a	V_a	-	-	V_a	-
		V_a^2	V_a^2	-	-	V_a^2	-	-	-	-
		VFA	VFA	VFA	VFA	VFA	VFA	-	VFA	-
		VFA^2	VFA^2	-	-	VFA^2	VFA^2	-	-	-
		logPen	-	logPen	Pen	logPen	Pen	Pen	-	Pen
		logA	logA	logA	logA	-	logA	logA	-	logA
		Density	Density	Density	Density	Density	Density	Density	Density	-
		V_{bit}	V_{bit}	V_{bit}	V_{bit}	V_{bit}	V_{bit}	V_{bit}	V_{bit}	-
		-	$T_{R\&B}$	-	-	$T_{R\&B}$	-	-	-	-
		G*	G*	G*	G*	-	G*	G*	-	G*
R^2	**ITS $_{dry}$**	0,58	0,59	0,57	0,57	0,55	0,56	0,54	0,51	0,17
	ITS $_{wet}$	0,61	0,63	0,61	0,59	0,52	0,59	0,56	0,47	0,13
	ITSR	0,61	0,67	0,67	0,68	0,63	0,66	0,49	0,40	0,16
R^2	ITS $_{dry}$	0,55	0,59	0,54	0,54	0,52	0,51	0,50	0,45	0,17
	ITS $_{wet}$	0,61	0,62	0,61	0,59	0,51	0,59	0,56	0,47	0,13
	ITSR	0,72	0,67	0,70	0,71	0,71	0,71	0,56	0,47	0,16

The maximum R-squared value, in the case where the individual ITS values are the target, is 0,59 and 0,63 for the dry and wet respectively, found by set 12. On the other hand, when the target is their combined ratio ITSR, the maximum is 0,72 found by set 11. It is clearly observed that the two targets have different predictabilities, despite their connection. It is also observed that the big increase between set 7 and 8 is not entirely depended to the addition of G*, but it is also the result of the exclusion of work 3.

At this point, a comparison of the results with the ones obtained by Mr. Florio's research should be made. At the time of his research works 1 and 2 were available, whereas at this point works 3 and 4 are added. What is more, water sensitivity was not thoroughly looked into using ITSR, but only the dry ITS values, due to time restrictions. Having these in mind, the comparison of the R-squared values obtained can be made.

The highest value found by his research was 0,76, which is fairly acceptable. In our case the highest value regarding the dry ITS was 0,59. Despite the addition of extra data points with work 4 (work 3 was not included in the set resulting to 0,59 because of the G* missing), the quality of the fit did not improve as one would expect, but on the other hand it decreased. A quite extensive analysis on the possible combinations of parameters was done, so this raises the doubt about the quality of the data available and their ability to explain this characteristic.

Even though sets 11 and 12 result in the highest R-squared values, they are not the ones preferred for final use. As explained, V_a and VFA taken into account two times, being squared the second time, has a redundancy issue and an unexplained physical use. For this reason, their applicability is doubted and not preferred. In addition, the less logarithms, the more "user friendly" and self-explained the relations are. These considerations lead to Set 14 as the most preferred, compromising part of the quality of the prediction, for an increase in usability. The multiplier terms obtained from the regression with ITSR as a target, and the back-calculated values they result in, are seen below:

Table 4. Parameter multipliers for set 14

	ITS_{dry}	ITS_{wet}
Intercept	-17,8580	-64,0318
V_a	-0,3614	-0,1621
VFA	-0,0531	-0,0562
Pen	-0,0147	-0,0798
logA	-8,8842	-13,9487
Density	3,4139	20,5334
G*	-0,0141	-0,0349
V_{bit}	1,4330	1,2980

Table 5. Measured vs Calculated ITSR values

$ITSR_{meas}$	$ITSR_{calc}$
96%	95%
78%	83%
93%	90%
87%	84%
93%	95%
106%	95%
86%	89%
97%	94%
91%	91%
80%	84%
89%	87%
97%	102%
91%	94%
85%	86%
103%	104%

Another way of getting an image about the quality of a fit is plotting the measured values against their corresponding calculated ones, and assessing their position relating to the x=y line. The closest the points to the line, the better the fit. In the case of ITSR, we get a fairly acceptable scatter around the equality line, seen below in the figure.

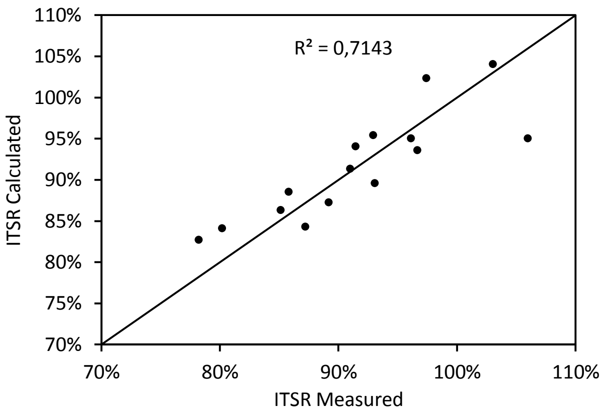

Figure 1. Measured vs Calculated ITSR

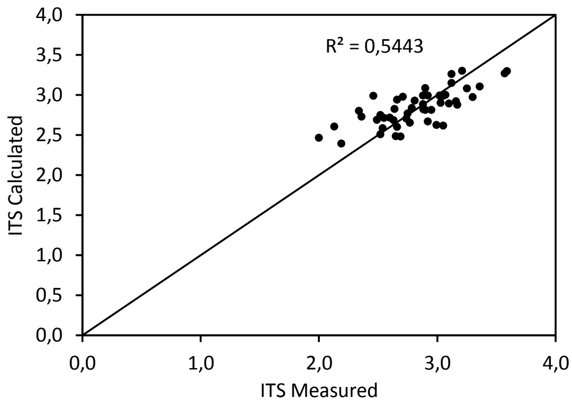

Figure 2. Measured vs Calculated ITS_{dry} values

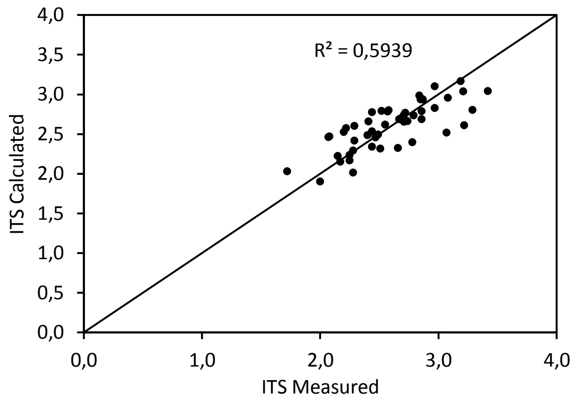

Figure 3. Measured vs Calculated ITS_{wet} values

In the case of ITS for wet and dry, even though the R-square values do not seem to be statistically acceptable, the scatterplot with the line of equality give a quite good image about the fit.

2.3 Comparison of Lab to Field measured properties

2.3.1 Data analysis

Initially, the tool used to compare the lab to the field measured properties was the scatterplot with the equality line, previously used to check the accuracy of measured to calculated values. This plot can be seen below, comparing all the lab ITS values (F1) to the field (F3), distinguishing them between wet and dry.

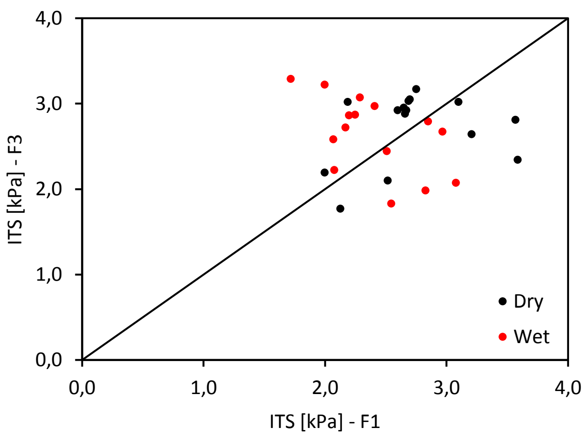

Figure 4. Lab vs Field ITS values (distinguished by conditioning)

It can be seen that the correspondence cannot be considered very accurate. Most of the points lie far from the equality line.

However, this method proved to be not the ideal for this kind of comparison. The scatter depends on the correspondence of x-values to y-values, in our case lab to field, where in reality there is no such correspondence. The ITS values provided in the data set refer to different specimens in the lab and different in the field, meaning that their properties might differ. Putting the values in a different order will result in a different plot, making this a rather subjective method.

An appropriate tool of comparing in this case should not take into account individual points, but instead look at the general image and trend of the whole data set. This is achieved by boxplots, which is a way of graphically depicting groups of numerical data through their quartiles. They display variation in samples of a statistical population without making any assumptions of the underlying statistical distribution.

The first figure made up by the boxplots of the ITS values from all works, regardless of their conditioning phase. It depicts the general image of the tests. It is visible that field values with an average of 2,68 kPa are slightly bigger than the lab determined, being 2,56 kPa on average.

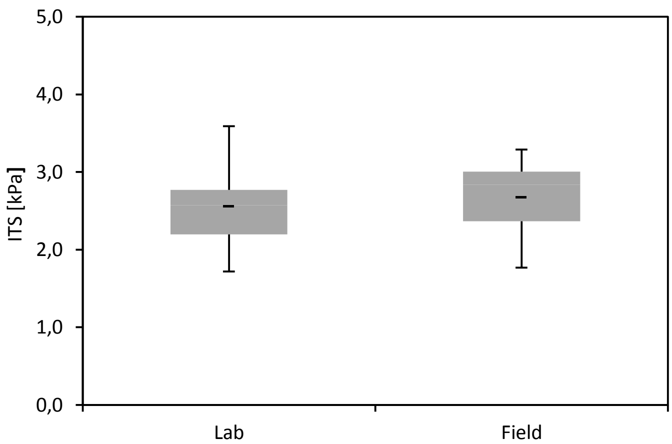

Figure 5. Boxplots for ITS lab and field values

Similar observations can be made by separating dry from wet specimens' ITS boxplots. Dry ITS values determined in the field have a distribution lying slightly higher than the field specimens. As for the wet, in general they are lower than they dry values, and also have the same relation between lab and field. In this case though, the difference between them is bigger and more obvious.

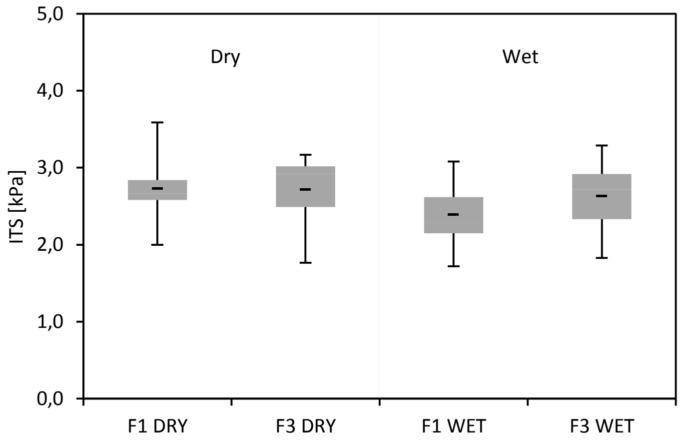

Figure 6. Boxplots for ITS lab and field values, separated by conditioning

Making the same comparison, this time with ITSR as the criterion, we get the same image, seen in the column chart below. Average ITSR values determined by all works, are significantly higher in the field than in the lab. This means that lab specimens are more susceptible to moisture problems than the field ones, meaning that this performance criterion is more likely to be met.

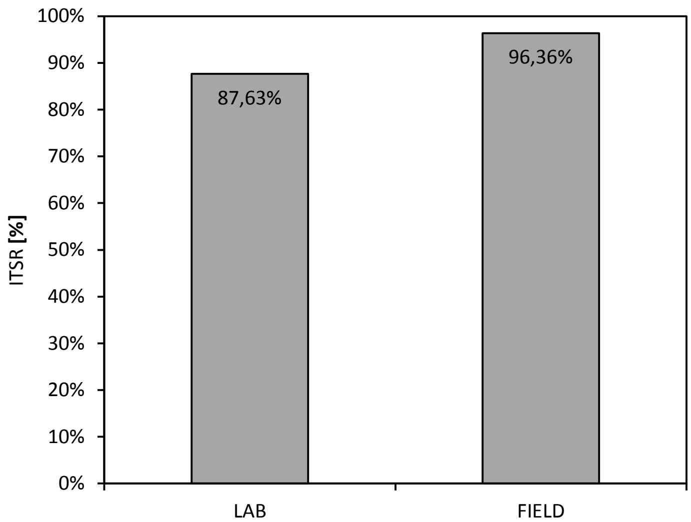

Figure 7. Lab vs Field ITSR averages

If we look at the different works separately in the following figure we can draw some more specific conclusions regarding the contractor's accuracy. The closest achieved result is in Work 3 by contractor Van Der Lee, where the lab and field values differ by less than 1%. The lowest relation is seen in Work 4 where lab specimens ITSR value is 17% lower than the field, with the lowest F1 value of all, at 80,12%. Work 1 also shows a considerable difference between F1 and F3, while Work 2 is at a good level of correlation.

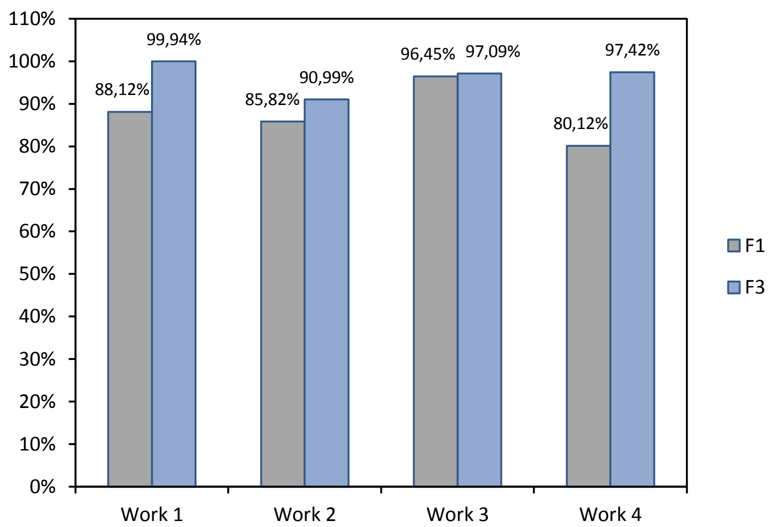

Figure 8. Lab vs Field ITSR averages per work

2.3.2 Explanatory factors

In order to look deeper into this comparison and trace probable causes of the deviating properties determined in the lab, the volumetric properties and design characteristics of the different works have to be studied. For this reason, the mixtures densities were chosen as the property that would possibly explain these differences better. As it was stated in previous chapters, it has a known effect on moisture susceptibility, and on top of that, it is the most difficult to achieve accurately in terms of target density, due to the high sensitivity and dependency in compaction conditions.

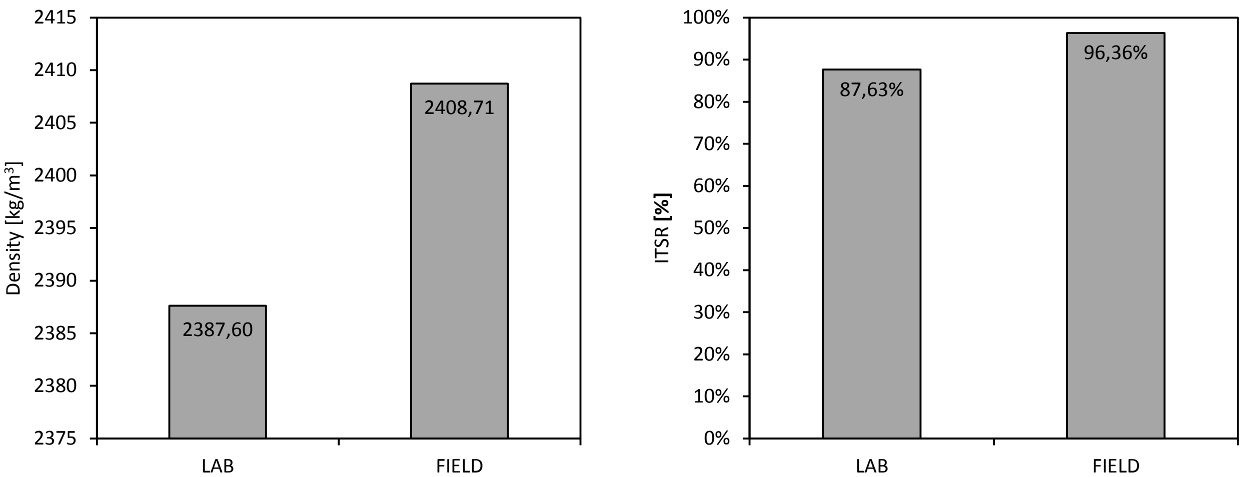

Figure 9. Average Densities and Average ITSR in Lab and Field

It is clear that the lower densities achieved in the lab lead to lower ITSR values, thus higher water damage susceptibility. The individual works comparison between densities and ITS is seen below. The dashed lines refer to the target density (red) and the upper limit of the ±30 kg/m^3 threshold (grey).

Work 1

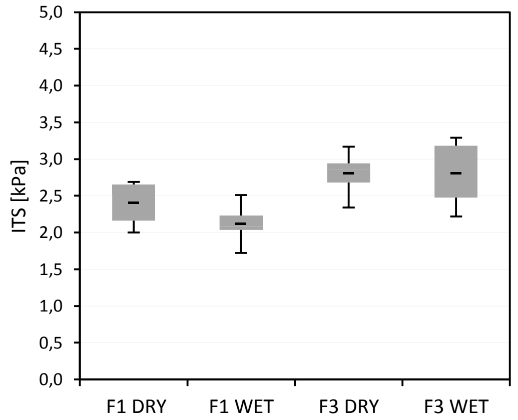

Figure 10. Work 1 - ITS per phase and conditioning

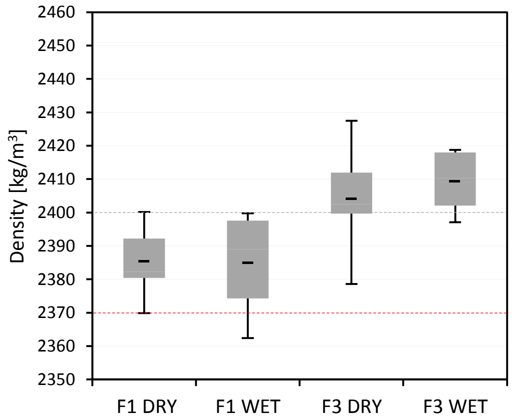

Figure 11. Work 1 - Densities per phase and conditioning

Looking at Work 1 we can see that densities in the field are higher even from the upper limit of the acceptable error. The overcompaction effect is visible in the ITS values which are higher, for both conditioning phases, in the field. In addition, not only are they higher, their ratio is also higher (99,94% vs 88,12% seen in figure 8). This leads to the observation that highly compacted specimens perform better under moist conditions.

Work 2

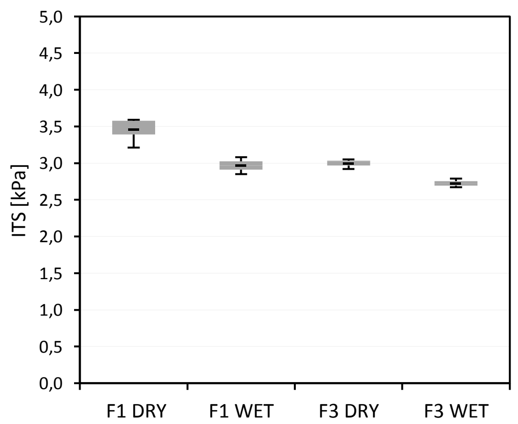

Figure 12. Work 2 - ITS per phase and conditioning

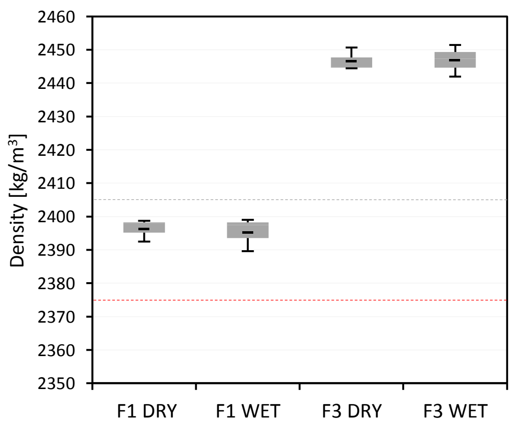

Figure 13. Work 2 - Densities per phase and conditioning

Work 2 is the most "unconventional" of all, in terms of Density-ITS relation. Field specimens show the highest compaction of all, almost 100 kg/m^3 above the target, comparing to lab values which are within the limits. However, contrary to the image seen in work 1, ITS values follow a different trend, being higher in the lab. Even though the ratio in F3 might be better (90,99% vs 85,82%), the absolute values are lower. This inconsistency with the densities leads to investigating other factors that lie behind. Indeed, looking back in the data set, bitumen stiffness at f=0,1 rad/s is immensely higher in the lab (figure 18), despite the fact mixtures in the same work were designed with the same properties. A different type of bitumen was apparently used. This fact could possibly explain the higher ITS with the lower density being compensated by the bitumen's stiffness.

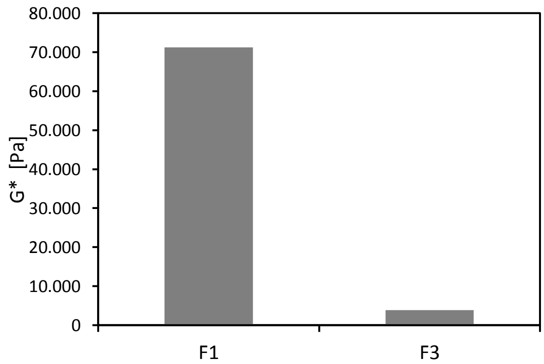

Figure 14. Bitumen stiffness G* at f=0,1 rad/s for Work 2

Work 3

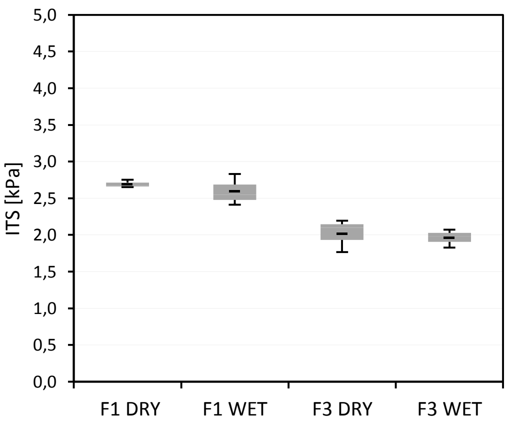

Figure 15. Work 3 - ITS per phase and conditioning

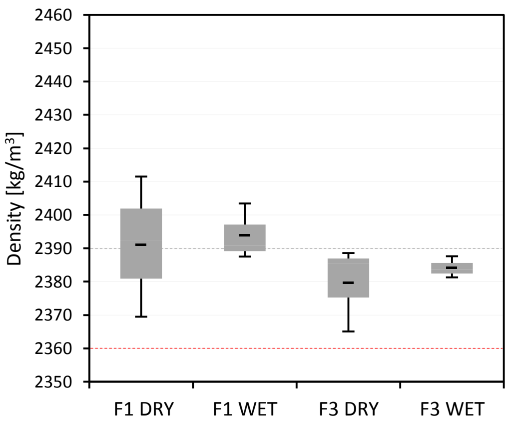

Figure 16. Work 3 - Densities per phase and conditioning

The same pattern as in work 1 is observed in work 3, with density and ITS values positively related. In this case though, field densities are lower, lying within the target limits, while the lab densities are slightly over it. The ratios are almost identical, with less than 1% of difference. However, the absolute values in the lab are higher, meaning that in the end, in terms of performance, the lab specimens are considered better.

Work 4

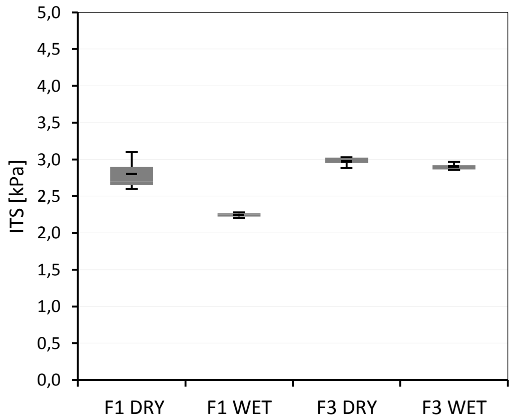

Figure 17. Work 4 - ITS per phase and conditioning

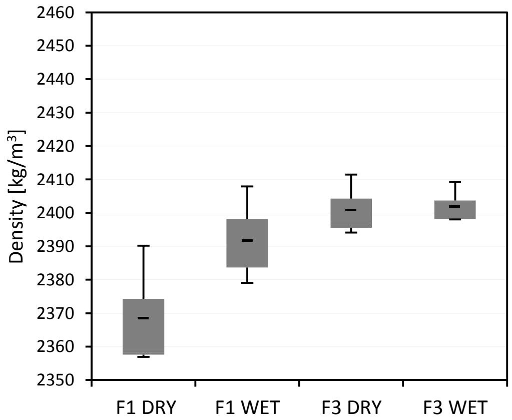

Figure 18. Work 4 - Densities per phase and conditioning

In the case of work 4, target densities were not provided, but the comparison between their values can still be made. Slightly overcompacted field specimens show a bit higher ITS values with a ratio of 97,42%. This ratio is much bigger than the lab's which is 80,12%, and is the lowest of all works. It is a significant observation at this point that the lab densities in this work differ between dry and wet specimens. In all the works, dry and wet specimens have almost the same density (maximum deviation 5kg/m^3), despite the fact that densities between F1 and F3 have deviations. This is not the case in work 4, where dry specimens' density is more than 20 kg/m^3 lower from the wet's. However, this still does not comply with the trend that higher density leads to higher ITS, and makes it more complicated meaning that only density cannot justify the test results.

2.3.3 Conclusion

In general, the correlation between lab and field determined water damage resistance can be considered low. Specimens extracted from the field performed much better in terms of Indirect Tensile Strength Ratio, but also in the most cases in terms of absolute Indirect Tensile Strength values in the wet and dry conditioning phases.

This deviation is quite well explained by the inaccuracies in compaction and target density achievement. Almost all categories were not acceptably close to the target density, with the field specimens being in many cases over-compacted. This stresses the issue of compaction procedures accuracy, firstly in the field, and at a lower rate in the lab. Even though in the case of moisture susceptibility this inaccuracy in compaction works in favour, it will later be seen that in other properties it has a negative effect.

Of course, there are also other factors in the mixture design and production that affect water damage in different ways, hence this complexity makes it very difficult to model it with an accuracy. However, since as explained, density has a big influence and even more sensitivity to small changes, it can be a fairly good indicating factor in the comparison between field and lab determined properties.

3. PERMANENT DEFORMATION

3.1 Literature Review

3.1.1 Definition

Permanent deformation in a pavement layer is a very common phenomenon and causes the development of ruts along the wheel path at the surface. Hence, when talking about permanent deformation, we talk in terms of rutting.

Rutting is defined as a longitudinal surface depression occurring in the wheel paths of roadways. It is often followed in later stages by an upheaval along the sides of the rut [5]. Rutting accumulates incrementally with small permanent deformations from each load application (i.e. each wheel pass) over the pavement's service life and is by definition a load-related pavement distress. It is a high temperature phenomenon, i.e. most often occurs during the summer when high pavement temperatures are evident. Its importance in the pavement performance lies in the fact that it can lead to structural failure and potential danger from hydroplaning [6].

Figure 19. Severe type-b Rutting due to lateral flow [7]

3.1.2 Types of rutting

There are three types of rutting that are distinguished by the cause and the layer in which they appear.

a) One-dimensional densification or vertical compression

A depression near the centre of the wheel path without an accompanying hump on either side of the depression is caused due to material densification. This densification is generally caused by excessive air voids or inadequate compaction after the placement of the asphalt layer. In this way the material is allowed to further compact when it is subjected to traffic load. This type of rutting usually results in a low to moderately severe levels of rutting.

b) Lateral flow or plastic movement

This type is caused by the localized shear failure by overstressing the pavement with high tire pressure. A depression near the centre of the wheel path with humps on either side of the depression is caused by lateral flow. It occurs in mixtures with inadequate shear strength or an insufficient amount of total voids in the asphalt layer. In such cases lateral flow occurs because the low voids allow the asphalt to act as a lubricant rather than a binder. It is higher at higher temperatures, and less on highways with higher speeds due to the visco-elastic behaviour of asphalt. This type of rutting usually results in moderate to highly severe levels of rutting and is most difficult to predict.

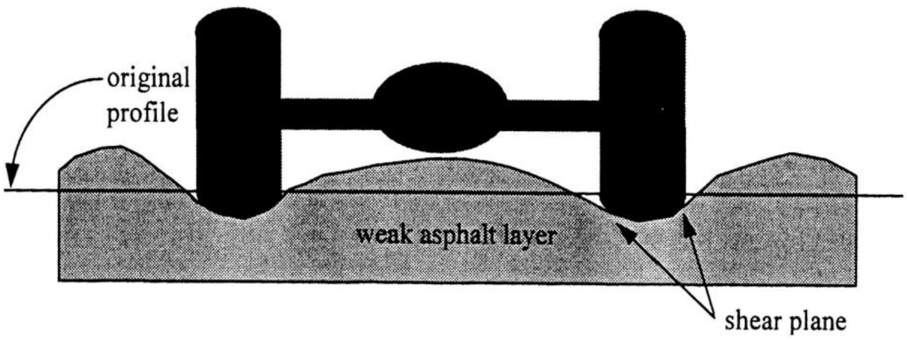

Picture 2. Rutting caused by weak asphalt layer [8]

c) Mechanical deformation

This third type of rutting is related to the unbound materials below the asphalt surface and their consolidation, densification, and/or lateral movement. It is a result of subsistence in the base, subbase or subgrade and is usually accompanied by a longitudinal cracking pattern at the pavement's surface, in the case of very stiff mixtures. There longitudinal cracks generally occur in the centre and along the outside edges of the ruts. [9]

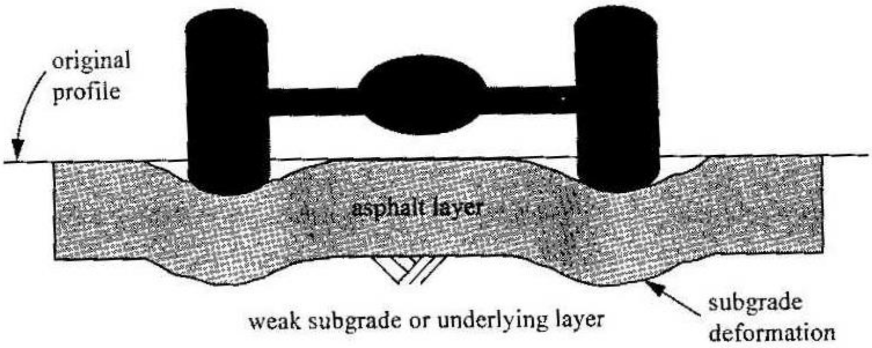

Picture 3. Rutting caused by weak subgrade [8]

3.1.3 Development stages

Rutting in asphalt layers develops in three stages (figure):

- *Primary (initial) stage* is related to the deformation caused by traffic compaction (densification, volume reduction) at the early stages of the pavement's service life (usually within the first year).
- *Secondary (middle) stage* is considered to be representative of the pavement's deformation behaviour for the greater part of its lifetime. Rutting rate is constant and is caused by horizontal and vertical traffic loads resulting in shear stresses in asphalt.
- *Tertiary (last) stage* is characterized by accelerated rutting and excessively rapid plastic deformations. [10]

The most common practice is rehabilitating the pavement prior to reaching the tertiary stage, since at that point rutting has already reached the regulation's threshold or another distress triggers the need for maintenance. For this reason, rutting modelling omits the last stage and is restricted to the secondary stage.

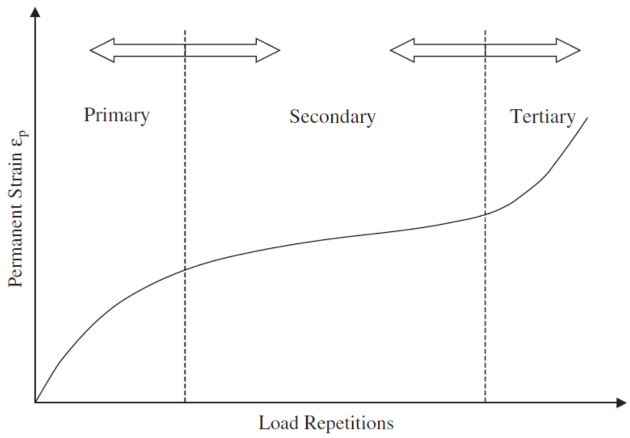

Figure 20. Rutting stages

3.1.4 Influencing factors

The permanent deformation of asphaltic mixtures is a complex phenomenon where the contribution of various components like the properties of the aggregates, bitumen, contact of aggregates and bitumen, etc. make up the overall performance. These properties are not constant but they are changing through time to the end of the pavement's service life, i.e. till the failure due to excessive permanent deformation or cracking. An overview of the various factors affecting the permanent deformation as well as effects of their changes are given in the table.

Table 6. Factors affecting rutting of asphalt mixtures [11]

Factor		Change in Factor	Effect of Change in Factor on rutting Resistance
Aggregate	Surface texture	Smooth to rough	Increase
	Gradation	Gap to continuous	Increase
	Shape	Rounded to angular	Increase
	Size	Increase in maximum size	Increase 1)
Binder	Stiffness 2)	Increase	Increase
Mixture	Binder content	Increase	Decrease
	Air void content 3)	Increase	Decrease
	Voids in the mineral aggregate 4)	Increase	Decrease
	Method of compaction	- 5)	- 5)
Test of field conditions	Temperature	Increase	Decrease
	State of stress/strain	Increase in tire contact pressure	Decrease
	Load repetitions	Dry to Wet	Decrease if mixture is water sensitive
	Water		

1) Assuming constant layer thickness.

2) Refers to stiffness at temperature at which rutting propensity is being determined. Modifiers may be utilized to increase stiffness at critical temperatures, thereby reducing rutting potential.

[3)]When air void content is less than about 3%, the rutting potential of mixture increases.
[4)]It is argued that very low (i.e. less than 10%) voids in the mineral aggregate should be avoided.
[5)]The method of compaction, whether laboratory or field, may influence the structure of the system and therefore the propensity for rutting

Apart from the overview seen above the bitumen properties and their relation to rutting were investigated in more detail for the research within NL-LAB. In particular, bitumen's stiffness expressed by G^* and bitumen's zero shear viscosity (*ZSV*) expressed by η_o were considered as parameters to be included in the rutting prediction.

- Bitumen Stiffness

  Stiffer binders at high service temperatures have less rutting. In general, the stiffer the asphalt binder, the stiffer the mixture and the more resistant to permanent deformation [12] (high G^* produces mixtures less susceptible to rutting [13]), which was also what was initially expected when considering the addition of this parameter. In the case of NL-LAB it was decided to work with the bitumen's stiffness at a low frequency level to approach the realistic loading conditions coming from the wheel passes. Hence the values at 0.1 rad/s (0.016 Hz) were used. The master curves where these values were taken from were constructed by DSR tests at 40^{o}C performed by TNO.

- Zero Shear Viscosity

  Looking into various studies regarding ZSV, the main conclusion was that ZSV (η_o) is a suitable indicator to evaluate the partial contribution of the bituminous binder to the rutting resistance of the asphalt pavement layers [14]. In particular, a good correlation of rutting rate and η_o was found for all the binders tested including unmodified and polymer-modified bitumen [15]. The advantage of ZSV comparing to G^* is that there is an apparent inability of G^* to capture the contribution to rutting resistance afforded by polymer modification [16]. In the case of pure binders, the correlation between this indicator and results from rutting tests on asphalt mixes is good. For Polymer modified binders on the other hand, it generally underestimates the resistance to rutting [17].

Literature regarding rutting and binder properties suggests that in order to characterize the rheological behaviour of a thermoplastic material in a certain temperature range, at least two properties should be estimated:

(a) consistency at a certain temperature (e.g. penetration Pen_{25} at 25^{o}C) or in a certain rheological state (e.g. softening point $T_{R\&B}$ or T_{800}) and

(b) temperature susceptibility (*PI*), or in the case of NL-LAB, A_{RTFO}, which is interrelated with *PI*.

$$PI = \frac{20 \cdot (1 - 25 \cdot A)}{1 + 50 \cdot A}$$

However, when using these parameters in a regression to predict a mixture's rutting behaviour, all three properties (Pen_{25}, $T_{R\&B}$ and A_{RTFO}) shall not be included at the same time due to their interrelation, thus only two of them might be included.

The above considerations were taken into account during the regression analysis for the prediction of functional properties at later chapters.

3.1.5 Brief test description

The test method followed in this project complies with the European Standards and is according to the guidelines specified in EN 12697-25:2013. This test method determines the resistance to permanent deformation of a cylindrical test specimen of a bituminous mixture by repeated load. During the test, the test's specimen change in height is measured at a specified number of loading cycles. From this, the cumulative axial strain ε_n of the specimen is determined as a function of the number of cycles. Out of the three methods described in the standard, the third method is used in NL-LAB, "Method B", which refers to the determination of creep characteristics of bituminous mixtures by means of triaxial cyclic compression test (TCCT).

The output of the test is related to two different methods described in detail in paragraph 3.2.2. The type test output includes the following parameters:

- Specimen code
- A_1 and B_1 coefficients, relating to the linear regression method
- A, B coefficients and f_c, relating to the power regression method
- ε_{1000}
- R^2

The minimum number of samples required for this test is three, which is what was also used in NL-LAB. The specimens were cylindrical, 80 mm thick and 100 mm in diameter, dimensions resulting from the nominal maximum aggregate size used in the mixtures. After the production and conditioning of the specimen according to the detailed procedures of the norm, it is placed in the apparatus.

The test is carried out by loading the specimen with a sinusoidal compressive stress in vertical direction, and a radial confining pressure, for the simulation of the confinement of the specimen within the pavement structure. The confining pressure is held constant throughout the test to simplify the test control. In reality though, there is a sinusoidal oscillation in the confining pressure with a certain phase lag in the vertical loading due to the viscoelastic properties of asphalt concrete. The test temperature for all tests was 40 °C.

It should be noted that the actual stress conditions in the road cannot be simulated in the laboratory with simple test equipment. They depend on time (position of the wheel), the road structure, the depth in the structure, the stiffness of other layers, among other aspects. Therefore, the applied load conditions are only an approximation of the loads that occur in reality. One might suggest that application of a cyclic confining stress is to be preferred over a static confining stress, which was used here. However, given the considerations mentioned in the standard and the fact that cyclic confining stresses require advanced and expensive equipment, it is not applied for type testing [18].

3.2 Permanent deformation prediction

3.2.1 MEPDG Methodology

The basis and starting point for the prediction of functional properties is the Mechanistic – Empirical Pavement Design Guide (MEPDG) also known as NCHRP Design Guide 1-37A. Report 580 titled "Specification Criteria for Simple Performance Tests for Rutting" refers to the concepts of permanent deformation. The rutting characteristics of HMA are obtained from a creep test, which is carried out at constant load between -10°C and -20°C. The mixture's properties along with the rutting characteristics measured are used as input in a regression analysis, leading to the rutting prediction formula. The differences from the Dutch method, which uses the triaxial cyclic compressive test and different test conditions, imply that some modifications need to be made to make the correspondence between the two methods and derive a prediction relation that applies to the Dutch conditions.

The Design Guide utilizes an approach that models the primary and secondary stage of rutting development, excluding the tertiary stage which is extremely time consuming and difficult to perform. The primary stage is modelled using an extrapolation of the secondary stage trend. It should be noted that the true plastic shear deformations are not modelled within the system. Another assumption is that chemically stabilized materials, bedrock and fractured slab materials are considered to have no contribution to the total permanent deformation of the system. Rutting is only estimated for asphalt bound and unbound layers.

Creep compliance which is used by the Design Guide is the ratio between the permanent deformation in time (*ε(t)*) and the constant stress applied (σ_{max}), and represents the inverse of the elastic modulus. It is represented in time as:

$$D(t) = D_1 \cdot t^m \quad (1) \qquad \text{and} \qquad D(t) = \frac{\varepsilon(t)}{\sigma} \quad (2)$$

where D_1 and m are fracture coefficients.

The relations that were derived after the regression analysis and suggested by the Design Guide to back-calculate D_1 and m are:

$$\log D_1 = -8{,}5241 + 0{,}01306 \cdot T + 0{,}7957 \cdot \log(V_a) + 2{,}0103 \cdot \log(VFA) - 1{,}923 \cdot \log(A_{RTFO}) \quad (3)$$

$$m = 1{,}168 - 0{,}00185 \cdot T - 0{,}01126 \cdot VFA + 0{,}00247 \cdot Pen_{77} + 0{,}001683 \cdot Pen_{77}^{0{,}4605} \cdot T \quad (4)$$

where,

T = Test temperature (^oF)

V_a = Air voids (%)

VFA = Voids filled with asphalt (%)

A_{RTFO} = Intercept of binder viscosity – temperature relationship for the RTFO condition

Pen_{77} = Penetration at 77 ^oF

The intercept of binder viscosity – temperature relationship is calculated as follows:

$$A_{RTFO} = \frac{\log Pen_{77} - \log 800}{25 - T_{R\&B}}$$

where,

Pen_{77} = Pen_{25} = penetration of bitumen at 77^oF (or 25^oC)

$T_{R\&B}$ = softening point of bitumen (^oF or ^oC)

3.2.2 NEN standard

As previously mentioned, the determination of the resistance of Asphalt Concrete to permanent deformation is done with a triaxial cyclic compressive test (TCCT) according to "EN 12697-25:Bituminous mixtures – Test methods – Part 25: Cyclic compression test". [18]

The creep curve that is generated from the test is a display of the cumulative axial strain, expressed in %, of the test specimen as a function of the number of loading cycles. Generally the following stages can be distinguished:

Stage 1: the (initial) part of the creep curve, where the slope of the curve decreases with increasing number of loading cycles.

Stage 2: the (middle) part of the creep curve, where the slope of the curve is quasi constant and can be expressed by the creep rate f_c. The exact turning point of the creep curve lies within this stage.

Stage 3: the (last) part of the creep curve, where the slope increases with increasing number of loading cycles.

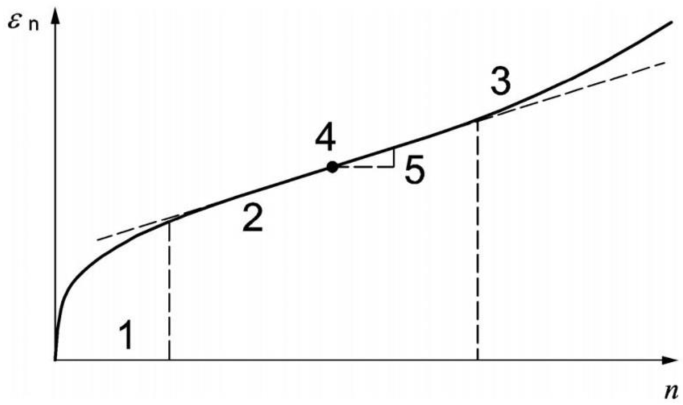

***Figure 21*. Creep curve [18]**

where,

ε_n = cumulative axial strain (%)

n = number of cycles

1 = stage 1

2 = stage 2

3 = stage 3

4 = turning point

5 = creep rate f_c (µm/m/loading cycle)

The resistance to permanent deformation of the mixture shall be determined by interpreting the creep curve, according to one of the following methods by minimizing the squared error between curve fit and measured deformation. There are two methods of interpreting the creep curve, both of which were utilized in this research.

- **Method 1**: Determination of the creep rate f_c.

If stage 2 is present the creep curve is represented on a linear scale, determining the slope B_1 from the least square linear fit of the (quasi) linear part of the creep curve (stage 2):

$$\varepsilon_n = A_1 + B_1 \cdot n \quad (5)$$

where,

ε_n = cumulative axial strain of the test specimen after n loading cycles, in percent (%) to the nearest 0,01%

A_1, B_1 = regression constants

The creep rate f_c in the (quasi) linear part of the creep curve in (µm/m/loading cycle) to the nearest 0,01 (µm/m/loading cycle) is:

$$f_c = B_1 \cdot 10^4 \quad (6)$$

The parameter f_c is used to characterize the resistance to permanent deformation of the mixture tested. This method has the disadvantage that it is only a poor representation of the creep curve. Furthermore, the creep rate f_c depends highly on the selected interval used for curve fitting, because there is generally no part with real constant slope in the creep curve.

- **Method 2**: Determination of the parameters B and $\varepsilon_{1000,calc}$

The (quasi) linear part of the creep curve is determined from the following least square power fit:

$$\varepsilon_n = A \cdot n^B + C \quad (7)$$

ε_n = cumulative axial strain of the test specimen after n loading cycles, in percent (%) to the nearest 0,01%

A = regression constant

B = power least square power fit or the slope from the least square linear fit on the log(ε_n-C) versus log$n$-values

C = factor to correct deformation at the beginning of the loading

The calculated permanent deformation after 1000 loading cycles, $\varepsilon_{1000,calc}$, in percent (%) to the nearest 0,01% is:

$$\varepsilon_{1000,calc} = A \cdot 1000^{B} + C$$

The parameters B and $\varepsilon_{1000,calc}$ are used to characterize the resistance to permanent deformation of the mixture. [18]

3.2.3 Correspondence of MEPDG and NEN

- **Method 1**

An initial assumption that needed to be made before the analysis, was necessitated by the data available in the contractors' test output files. The data related to permanent deformation included only the f_c values, meaning that the relation describing the creep curve had to be limited only to B_1 coefficient, neglecting the offset A_1. In this way, relation (5) becomes:

$$\varepsilon_n = B_1 \cdot n \;\;\rightarrow\;\; \varepsilon_n = \frac{f_c}{10^4} \cdot n \quad (8)$$

Due to the fact that the triaxial tests were performed with a cycle time of 1 second, the assumption that t = n is justified. Elaborating on relations (1) and (2) we get:

$$\frac{\varepsilon_n}{\sigma} = D_1 \cdot t^m \;\;\overset{t=n}{\rightarrow}\;\; \varepsilon_n = \sigma \cdot D_1 \cdot n^m \quad (9)$$

The goal is to be able to compare (8) to (9). The problem in this case is their form; relation 8 is in linear form whereas relation 9 is in power. The way to manipulate the relations and transform them into comparable forms, is taking the logarithm of all components of the relations:

$$(7):\;\; \log(\varepsilon_n) = \log(f_c \cdot 10^{-4}) + \log(n)$$
$$(8):\;\; \log(\varepsilon_n) = \log(\sigma) + \log(D_1) + m \cdot \log(n) = \log(\sigma \cdot D_1) + m \cdot \log(n)$$

The two relations can now be compared by corresponding their terms as follows:

$$\log(f_c \cdot 10^{-4}) = \log(\sigma \cdot D_1) \;\;\rightarrow\;\; \log(D_1) = \log\left(\frac{f_c \cdot 10^{-4}}{\sigma}\right)$$
$$m = 1$$

In this relation, f_c is known from the test output and σ_{max} is constant and is known from the test conditions. The right-hand side of the relation is in this way known.

Knowing from the Design Guide relation 3 that gives a prediction for $logD_1$ the correlation of D_1 and f_c can now be made by determining a new set of regression coefficients based on our set of data. Hence the regression analysis will be based on the following measured and calculated relations:

$$\log(D_1)_{measured} = \log\left(\frac{f_{c,measured} \cdot 10^{-4}}{\sigma_{\max}}\right)$$
$$\log(D_1)_{calculated} = \beta_o + \beta_1 \cdot T + \beta_2 \cdot \log(V_a) + \beta_3 \cdot \log(VFA) + \beta_4 \cdot \log(A_{RTFO})$$

The properties taken into consideration are the ones suggested by the Design Guide. They are used as at the preliminary phase of the regression. More properties are added or excluded at later stages to assess their effect on the quality of the fit. Their influence and how they were chosen is discussed in the next chapter.

After the $log(D_1)_{calculated}$ values are obtained, the goal of the analysis which is the value of f_c is back-calculated from:

$$f_{c,calc} = \left(\sigma_{\max} \cdot 10^4\right) \cdot 10^{\log(D_1)_{calc}}$$

The quality of the fit is determined by the calculation of R^2 from the values of $f_{c,meas}$ and $f_{c,calc}$.

- **Method 2**

Starting from the same point of the Design Guide, elaborations were needed to make the correspondence between relations (7) and (9). The task in this case was easier, because both relations are in a power form. The assumption of t=n is also valid in this case.

$$(7) \rightarrow \varepsilon_n = A \cdot n^B$$
$$(9) \rightarrow \varepsilon_n = \sigma_{\max} \cdot D_1 \cdot n^m$$

Then we get the following equations:

$$A = \sigma_{\max} \cdot D_1$$
$$B = m$$

The predicting relation the Design Guide suggests for D_1, is in logarithmic form, thus the first relation has to be firstly transformed in logarithmic before back-calculating A. Maximum stress σ_{max} is constant so the following relations can be used:

$$\log(D_1)_{measured} = \log\left(\frac{A_{measured}}{\sigma_{max}}\right)$$
$$\log(D_1)_{calculated} = \beta_o + \beta_1 \cdot T + \beta_2 \cdot \log(V_a) + \beta_3 \cdot \log(VFA) + \beta_4 \cdot \log(A_{RTFO})$$

$$m_{measured} = B_{measured}$$
$$m_{calculated} = \theta_o + \theta_1 \cdot T + \theta_2 \cdot VFA + \theta_3 \cdot Pen + \theta_4 \cdot Pen^a \cdot T$$

After the back-calculation of *A* and *B*, $\varepsilon_{1000,measured}$ is back-calculated as well based on the A_{calc} and B_{calc}.

$$A_{calc} = \sigma_{max} \cdot 10^{\log(D_1)_{calc}}$$
$$B_{calc} = m_{calc}$$
$$\varepsilon_{1000,calc} = A_{calc} \cdot 1000^{B,calc}$$

The quality of the fit is determined by the calculation of R^2 from the values of $\varepsilon_{1000,meas}$ and $\varepsilon_{1000,calc}$.

3.2.4 Analysis and results

- **Method 1**

Being the first regression analysis as part of this internship, the experience in the choice of parameters and their combination was still low. Hence the parameter sets shown in the table below are not the most complete in terms of possible combinations.

The data included in this analysis are limited to Work 1 only, so the advantage of having access to a big number of data was not taken at its full in this case. The rest of the works, even though they were already tested, were not yet extracted from the contractors' test reports at the time of the analysis. They were requested to be extracted and added to the available data, and were included in the next analyses.

The first analysis was carried out with the parameters suggested by the Design Guide, in the same form, giving a moderate R-square value (Set 1). Mixture density along with air void content have a direct impact on rutting, due to the first rutting type, of material densification at its early stages. Hence it was included in Set 2. Additionally, penetration grade and bitumen were also included due to their explained connection to rutting. The quality of the fit was improved, but still in moderate R-square values. After this addition, the choice of parameters was done mainly to assess the effect of the form in which the values enter the relation. As expected, whether temperature is taken in

Fahrenheit or in Celsius, does not affect the quality of the fit, since the relative variation remains the same. Looking into the effect of logarithmic values, the outcome was also that a parameter value taken in its linear form or in its logarithmic does not have an effect on the prediction quality. Set 9 draws the conclusion that $logA_{RTFO}$ is also independent of its form, and even not using the logarithm leads to the same result. In general the rest R-square values were in the range of 0.50, meaning that the fit would not be acceptable for use.

***Table 7.* Parameter Sets Overview for Method 1**

Set	1	2	3	4	5	6	7	8	9
	T (in ^oF)	T (in ^oF)	T (in ^oC)	logT (in ^oF)	logT (in ^oC)	T (in ^oF)	T (in ^oC)	T (in ^oC)	T (in ^oC)
	$logV_a$	$logV_a$	$logV_a$	$logV_a$	$logV_a$	V_a	V_a	V_a	V_a
	logVFA	logVFA	logVFA	logVFA	logVFA	VFA	VFA	VFA	VFA
	logA	logA	logA	logA	logA	log A	logA	logA	A
	-	Density	Density	logDensity	log Density	Density	Density	Density	Density
	-	Pen	Pen	logPen	logPen	Pen	Pen	-	Pen
	-	V_b	V_b	V_b	V_b	V_b	V_b	V_b	V_b
	Intercept	Intercept	Intercept	Intercept	Intercept	Intercept	Intercept	Intercept	Intercept
R^2	*0,46*	*0,50*	*0,50*	*0,51*	*0,51*	*0,51*	*0,51*	*0,51*	*0,51*

The independent parameters' multipliers obtained for set 7 are as seen on the table below, giving the equation as seen:

Table 8. Parameter multipliers

Intercept	-166,007
T (in ^oC)	-4,766
V_a	-0,228
VFA	-0,055
logA	-108,421
Density	0,010
Pen	0,012
V_b	42,816

$$\log D_{1,meas} = -166.007 - 4.766 \cdot T - 0.228 \cdot V_a - 0.055 \cdot VFA - 108.421 \cdot \log A + 0.010 \cdot Density + 0.012 \cdot Pen + 42.816 \cdot V_b$$

Doing the elaborations previously described, the final f_c value is predicted and can be seen in comparison to the measured values in the table.

Table 9. Work 1 - Calculated vs Measured f_c values from Set 7

Phase	$f_{c,meas}$	$f_{c,calc}$
1	0,100	0,177
1	0,130	0,190
1	0,080	0,238
1	0,080	0,213
1	0,340	0,278
1	0,346	0,251
1	0,267	0,293
1	0,451	0,207
2	0,214	0,148
2	0,167	0,144
2	0,165	0,205
2	0,217	0,176
2	0,178	0,156
2	0,164	0,200
2	0,151	0,182
2	0,147	0,169
3	0,160	0,155
3	0,190	0,163
3	0,160	0,183
3	0,170	0,150
3	0,166	0,123
3	0,190	0,153
3	0,157	0,158
3	0,142	0,165
4	0,016	0,032
4	0,016	0,029
4	0,010	0,026
4	0,020	0,038
4	0,014	0,041

This moderate quality fit is also visible in the plot below. Y-axis refers to the back-calculated values from the regression and X-axis refers to the measured ones from the test. The diagonal depicts the equality line x=y. The closer the points to x=y, the better the quality of the fit. In ideal conditions, all points would fall on the line, giving R^2=1,00. Parameter Set 7 was chosen to visualize this fact because it would be the most appropriate and “user-friendly” among the nine sets. Temperature is in Celsius and all the parameters are used without a logarithm (logA is usually used with a logarithm).

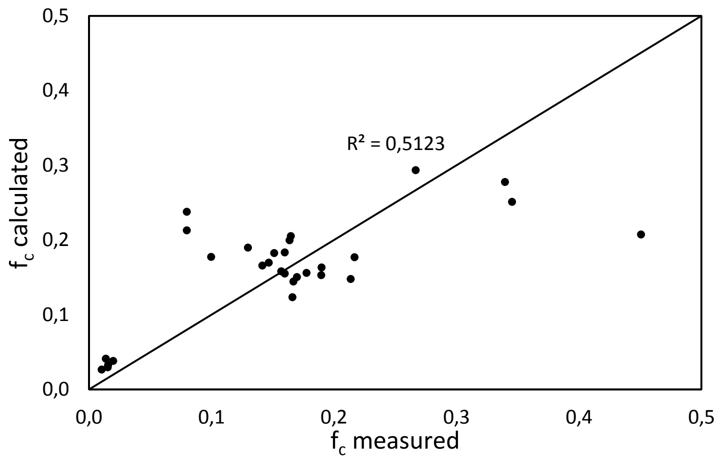

Figure 22. Parameter Set 7 Fit

Plotting the calculated *$logD_1$* values against the measured ones, which is one step before f_c, gives an image of a better fit. Indeed, the coefficient of determination for *$logD_1$* values is R^2=0,75 which is acceptable and far better than f_c. However, this is explained by the effect of logarithm, which diminishes big differences in the values and does not in fact represent the actual scatter. Removing the logarithm leads to the same fit found for the f_c values.

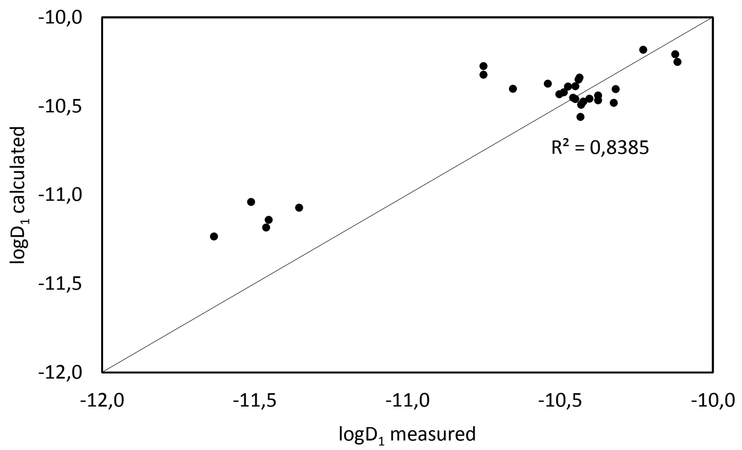

Figure 23. Measured vs Calculated logD1 for Set 7

– **Method 2**

In order to perform the analysis with Method 2 of NEN, the additional data needed were requested to be extracted from the type tests reports. This was carried out by TNO, obtaining eventually the test outputs including all the data needed.

Doing a more in-depth and elaborate combination of the parameters used, their effect was more extensively looked into, than it was in Method 1. The principle however of looking at different combinations and forms remained the same. Starting from the same point of the Design Guide for

$logD_1$, nine set of parameters were analysed. As far as *m* is concerned, the parameters that Mr. Berti used in his research were chosen as the starting point. The set was almost identical to the Design Guide's with the exception that the ϑ_5 parameter was excluded. This was done because the aim was to use a linear set of equations that could be solved by the readily available software. The term Pen_{77}^{a} from the expression required non-linear fitting of the coefficient *a*, which made the analysis more complicated [19]. *G** and *sinδ* values were also available and the term of ring and ball temperature, $T_{R\&B}$, was also tested. All the temperature values were used in Celsius ^{o}C.

The difference in this method is that both $logD_1$ and *m* had to be back-calculated, and their combination then used to back-calculate the target criterion, which was ε_{1000}. This means that a complicated and more time-consuming analysis was necessary.

Starting from the point described previously, density was added in Set 2 for the reason also explained in Method 1. No improvement was observed in the fit quality. Adding the term of bitumen stiffness *G** slightly improves the accuracy to 0,55, still standing below an acceptable value though. Due to the high *G** and density absolute values comparing to the rest of the properties, in order to keep them in the same range and have more user-friendly parameters, their values were divided by a factor of 10^3, only for visual reasons with no computational meaning. It should also be noted that *G** values for Work 3 were not available, hence the analysis where this property was included, did not take into account work 3 at all.

Including the phase angle *sinδ* decreased the accuracy of the prediction to 0,51, leading to its exclusion in the next sets. The replacement of the intercept of binder viscosity – temperature *logA* in the $logD_1$ parameters, with the softening point temperature $T_{R\&B}$ and the penetration value, leads to the best fit of the analysis with R^2=0,57. This replacement was done having in mind the suggestion that two of these three properties shall be used at once due to their interrelation.

Sets 6 and 7 assess the effect of the logarithmic values in the fit, instead of the linear, where no difference was eventually observed. In Set 8, *T*, V_a and *VFA* were excluded and no significant deviation was observed. Finally, in Set 9 the term $T_{R\&B}$**Pen* was added following the suggestion by Mr. Berti's research; no positive effect was seen in the quality of the fit. The overview of the parameter sets used is seen in the table below.

In general, R^2 values remained at a relatively moderate values again, no matter the combination of parameters and their explained physical significance in reality. What is more, with the inclusion of such a big data set (75 points comparing to 29 used in Method 1), one would expect a higher prediction accuracy, coming from the wider variability of the test results explained by the properties.

However, this is not the case when the dependent variables are not sufficiently explained by the independent, or when the data used are correlated which means further additions do not really add to the quality.

Furthermore, making a comparison with Mr. Berti's research, even though his dataset consisted of 39 data points, which is much less comparing to this dataset of 75, the quality of his fits is far better than the one found. This comes in contrast to what is normally expected, that the more data points lead to higher accuracy.

This draws the attention to trace the low quality fits back to the dataset, by investigating the accuracy and correctness of the tests performed and possibly looking deeper in the optimal parameter combinations.

Table 10. Parameter Sets Overview for Method 2

	SET 1		SET 2		SET 3		SET 4		SET 5	
	$logD_1$	m	$logD_1$	m	$logD_1$	m	$logD_1$	m	$logD_1$	m
	T	-	T	-	T	-	T	-	T	-
	$logV_a$	V_a	$logV_a$	V_a	$logV_a$	V_a	$logV_a$	V_a	$logV_a$	V_a
	logVFA	VFA	logVFA	VFA	logVFA	VFA	logVFA	VFA	logVFA	VFA
	logA	-	logA	-	logA	-	logA	-	-	-
	-	Pen	-	Pen	-	Pen	-	Pen	Pen	Pen
	-	-	Density	Density	Density	Density	Density	Density	Density	Density
	-	-	-	-	G*	G*	G*/sinδ	G*/sinδ	G*	G*
	-	-	-	-	-	-	-	-	TR&B	-
	-	-	-	-	-	-	-	-	-	-
R^2	*0,49*		*0,50*		*0,55*		*0,51*		***0,57***	

	SET 6		SET 7		SET 8		SET 9	
	$logD_1$	m	$logD_1$	m	$logD_1$	m	$logD_1$	m
	logT	-	T	-	-	-	T	-
	$logV_a$	V_a	$logV_a$	V_a	-	-	$logV_a$	V_a
	logVFA	VFA	logVFA	VFA	-	-	logVFA	VFA
	-	-	logA	logA	-	-	-	-
	logPen	Pen	logPen	Pen	Pen	Pen	-	-
	logDensity	Density	Density	Density	Density	Density	Density	Density
	G*	G*	G*	G*	G*	G*	G*	G*
	$logT_{R\&B}$	-	-	-	$T_{R\&B}$	-	-	-
	-	-	-	-	-	-	$T_{R\&B}$*Pen	$T_{R\&B}$*Pen
R^2	*0,51*		*0,50*		*0,53*		*0,49*	

The parameter multipliers that are calculated in Set 5 are seen in table 6 below. Table 7 gives the ε_{1000} back-calculated values in comparison to the measured ones.

Table 11. Parameter multipliers

logD1		m	
Intercept	4,38483	Intercept	-1,34155
Temperature	0,04504	Va	-0,03916
logVa	-0,13888	VFA	-0,00976
logVFA	5,13752	Pen	-0,00273
TR&B	-0,18402	Density	1,01105
Pen	-0,07487	G*	-0,00094
Density	-4,72367		
G*	0,03087		

$$\log D_1 = 4{,}3848 + 0{,}04505 \cdot T - 0{,}1388 \cdot \log(V_a) + 5{,}1375 \cdot \log(VFA) - 0{,}184 \cdot T_{R\&B} - 0{,}0748 \cdot Pen_{25} - 4{,}7236 \cdot Dens + 0{,}0308 \cdot G^*$$

$$m = -1{,}3415 - 0{,}0391 \cdot V_a - 0{,}00976 \cdot VFA - 0{,}00273 \cdot Pen_{25} + 1{,}011 \cdot Dens - 0{,}00094 \cdot G^*$$

Table 12. Measured vs Calculated ε_{1000} values

$\varepsilon_{1000,meas}$	$\varepsilon_{1000,calc}$	$\varepsilon_{1000,meas}$	$\varepsilon_{1000,calc}$	$\varepsilon_{1000,meas}$	$\varepsilon_{1000,calc}$
0,46	0,49	0,65	0,86	0,49	0,34
0,52	0,51	0,69	0,89	0,63	0,33
0,39	0,58	0,32	0,31	0,53	0,31
0,48	0,54	0,36	0,31	0,66	0,56
0,62	0,62	0,17	0,31	0,78	0,61
0,96	0,59	0,13	0,33	0,84	0,61
0,71	0,64	0,14	0,33	0,92	0,67
0,93	0,52	0,46	0,59	0,66	0,59
0,56	0,69	0,46	0,61	0,39	0,56
0,53	0,68	0,45	0,62	0,57	0,53
0,46	0,82	0,47	0,58	0,26	0,65
0,46	0,76	0,45	0,66	0,93	0,68
0,53	0,69	1,91	1,84	1,94	0,92
0,46	0,80	1,78	1,92	1,97	0,88
0,53	0,76	1,53	1,73	2,00	1,02
0,44	0,73	1,63	1,78	1,99	1,06
0,67	0,87	2,14	1,76	0,95	1,42
0,90	0,90	0,61	0,77	1,42	1,18
1,01	0,99	0,67	0,70	1,04	1,46
0,82	0,85	0,61	0,65	1,04	1,23
0,58	0,73	0,54	0,82		
0,82	0,84	0,65	0,28		

Even though looking at the R^2 values we come to the conclusion drawn above, plotting the measured versus the predicted values from Set 5, gives an image of a much better quality fit. Comparing also to the same graph from Method 2 (Figure 4), this conclusion is enhanced.

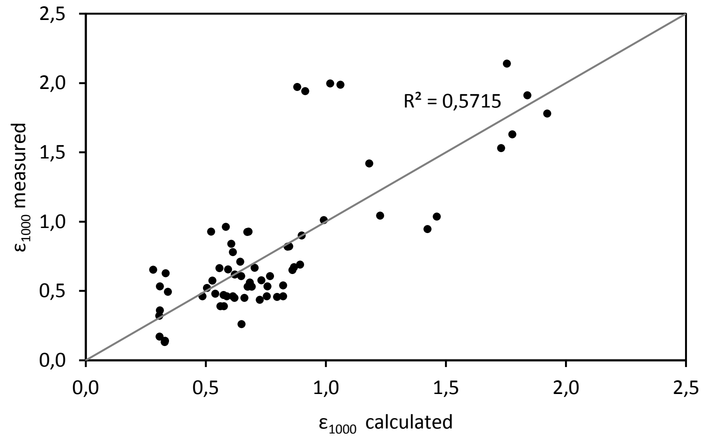

Figure 24. Parameter Set 5 Fit

This enhancement of the visual representation of the fit is also seen in the plotting of the creep curves seen below, depicting the creep curve generated from the *A* and *B* parameters of a randomly chosen test (equation 7). Even though with increasing loading cycles the strain values start to deviate, this deviation is at levels not very big, having also in mind that even the measured rutting relation gives an estimation of the creep curve and not the actual curve.

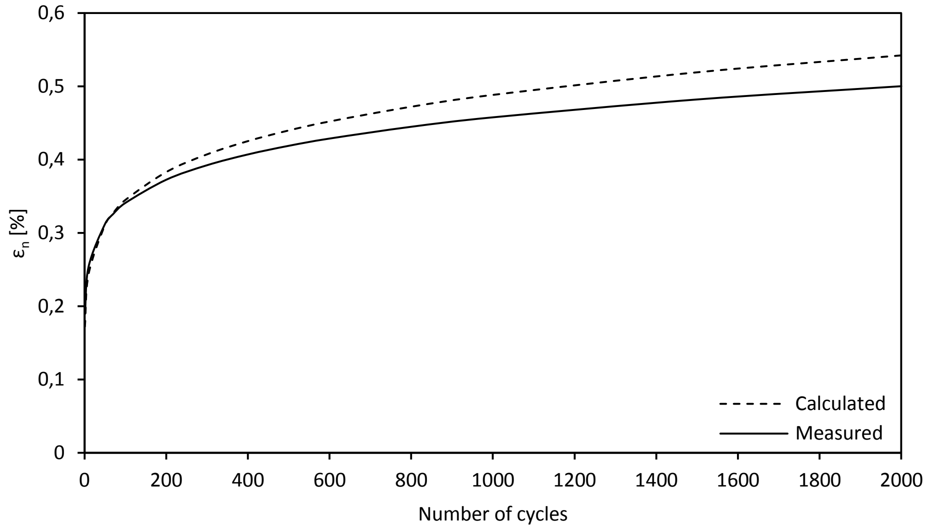

Figure 25. Representative measured vs calculated rutting curves

3.3 Comparison of Lab to Field measured properties

3.3.1 Data analysis

The comparison was carried out employing the same statistical tool as in water sensitivity, the boxplots. The difference in this case was that not only one method is used to characterize rutting resistance, but as mentioned before, two methods; method 1 relating to strain rate f_c, and method 2 relating to permanent strain ε_{1000}. For this reason both of them were plotted. In addition, phase 4 relating to the aged field specimens was made available at this point and was included in the comparison. The boxplots of the two properties are seen below for all works.

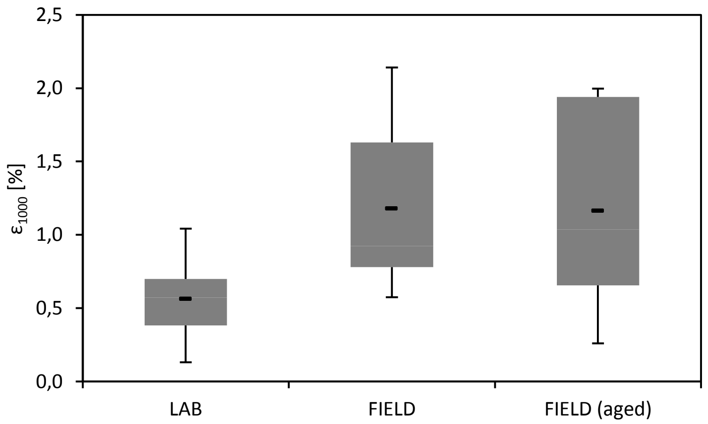

Figure 26. F1vsF3vsF4 Permanent strain comparison

In general, it is obvious that specimens from the lab (F1) show significantly lower strain levels than those from the field (F3), almost two times lower. As far as the aged specimens are concerned, one would expect them to show a lower permanent deformation, coming from the ageing effect which leads to bitumen hardening, and consequently harder mixture. Even though this expectation is slightly fulfilled, looking at the mean values of the boxplots (0,118 vs 0,116), the distribution of the values around the mean do not follow this rule.

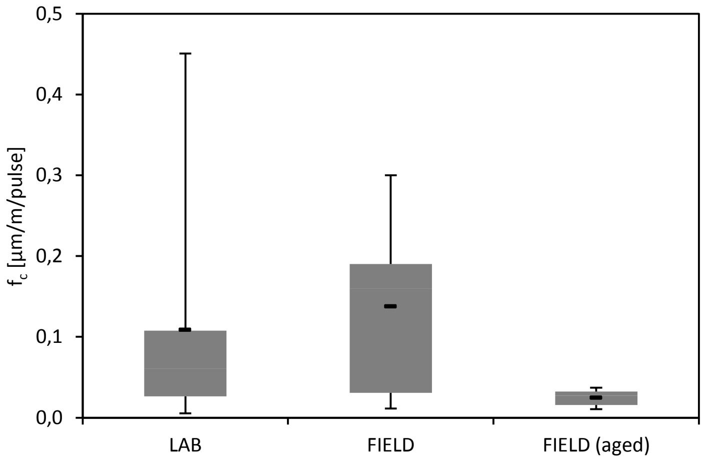

Figure 27. F1vsF3vsF4 Strain rate comparison

Looking at the strain rates, the image is the same for lab and field specimens as before. Mean values in F1 are clearly lower than F3. A notable point is the immensely high scatter of some values in F1, reaching values more than 4 times higher than the mean. All 4 values that lead to this distribution are from Work 1, Lab 2 (MNO) and are possibly outliers. It needs to be investigated whether they should be excluded from the data set due to possible defects in the test or analysis.

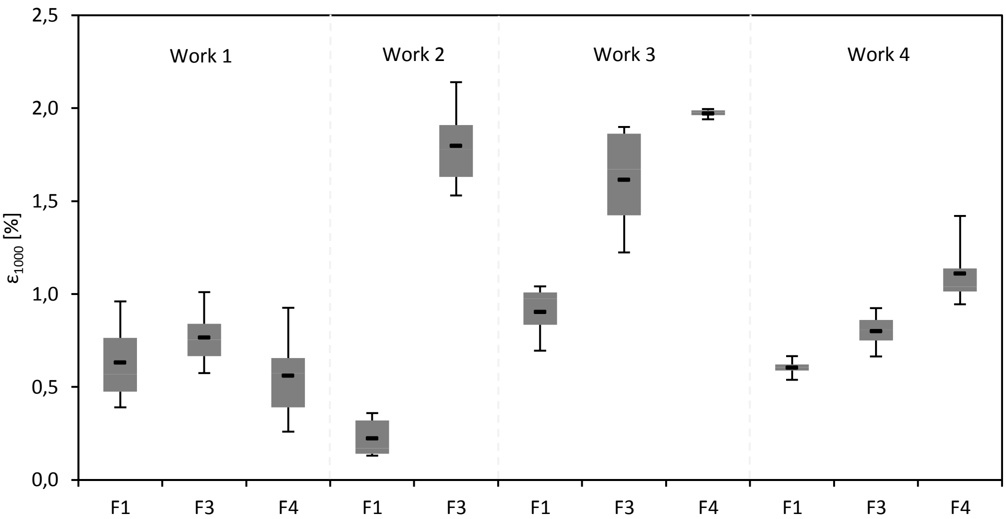

Figure 28. Individual works – Strain levels comparison

The figure above contains the boxplots of the individual works' permanent strain levels. Some observations that can be made on this figure are:

- Work 1: F1 values lie slightly lower than F3 and follows the general trend of figure 8. F4 however is what we initially expected for aged specimens. It shows the lowest strain level of all, resulting possibly from the improvement of the mixture's rutting resistance due to bitumen hardening.

– Work 2: Lab specimens of this work show by far the lowest rutting levels of all works. Surprisingly though, field values are the second biggest. This peculiarity will be investigated in the next chapter. Aged specimens were not provided for this work.
– Work 3: Rutting values for F1 are relatively high comparing to other works. Comparing to F3 it is much lower, following the general trend of lab specimens showing better rutting performance than field specimens. Contrary to the expectations, F4 is higher than the other two phases.
– Work 4: The relation between the phases is similar to work's 3, but in lower rutting levels.

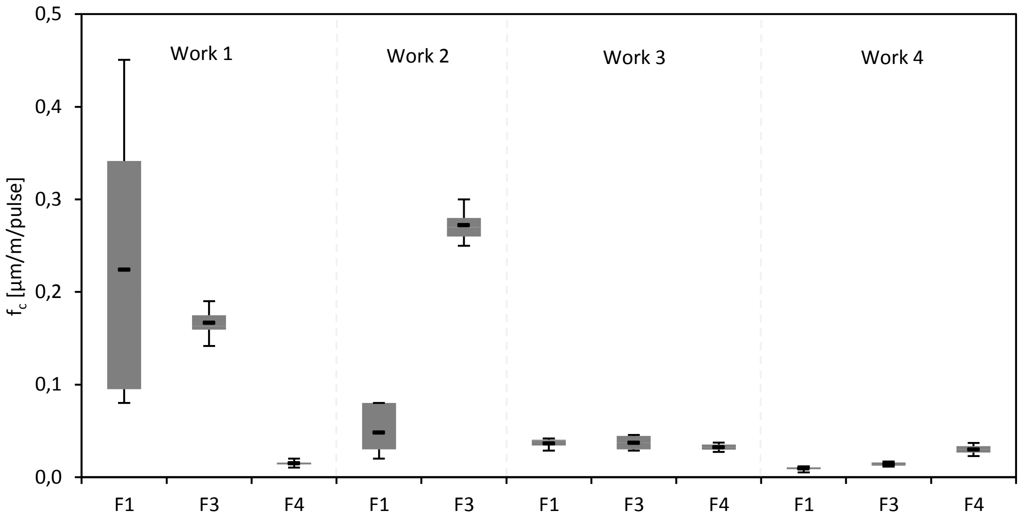

Figure 29. Individual works – Strain rates comparison

Plotting the same graph, this time for strain rates f_c, some observations can be made, which differ from the ones regarding the strain levels.

– Work 1: Lab specimens in F1 show the biggest f_c values, with a highly non-concentrated distribution around the mean value. This was also observed in figure 9. High rutting rates with low rutting levels can be related to a reduced rutting at the initial stages of a mixture's lifetime. Strain rates in F3 are clearly lower with a more concentrated scatter around the average. Aged specimens have ten times lower f_c values. The general trend of these values does not follow the corresponding trend of ε_{1000}.
– Work 2: The image is similar to the strain levels. f_c values of phase 1 are much lower than those of phase 3.

– Work 3: Strain rates for all works are relatively low. The mean values of F1 and F3 are the same, whereas F4 is slightly lower (0,037 vs 0,034).
– Work 4: Strain rates here are the lower of all works. Lab specimens show values a bit lower than the field ones. Aged specimens however show a considerable increase in strain rates (from 0,014 to 0,030).

In general, there is no visible and consistent trend in the relation between lab and field specimens rutting behaviour, whether it is about strain levels or strain rates. Furthermore, high strain levels does not necessary mean high strain rates. This necessitates a further investigation in the source of these inconsistencies, back in the mixtures volumetric characteristics.

3.3.2 Explanatory factors

The inconsistency described in the previous chapter needs to be studied in more detail to name possible reasons and identify peculiarities in the test data. This is done by plotting boxplots for some main mixture design characteristics i.e. density, void content, bitumen content and bitumen stiffness, that have a known effect on rutting behaviour. These plots can be seen below. The red dotted lines in the density graph represent the target density of each work and the upper limit of ±30 kg/m^3 threshold.

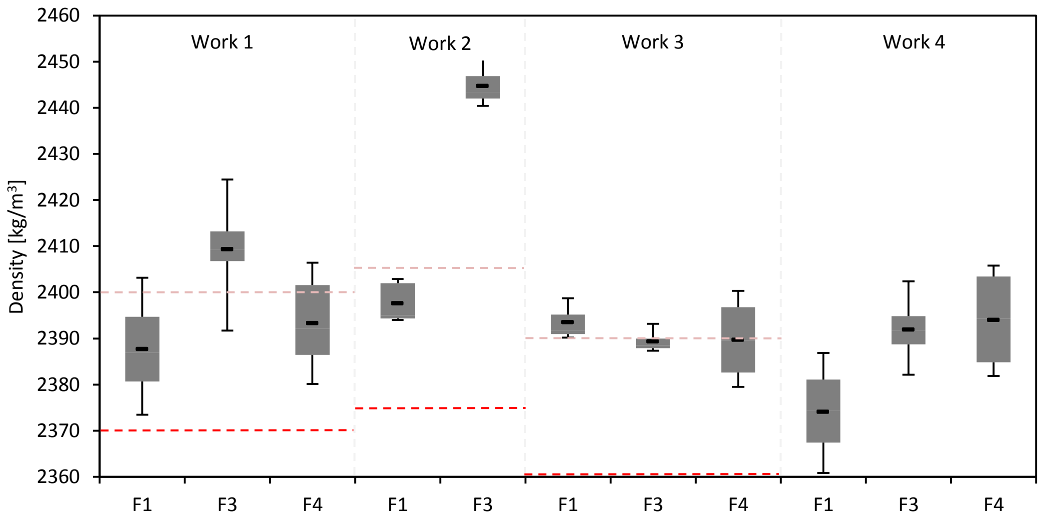

Figure 30. Individual densities per work and phase

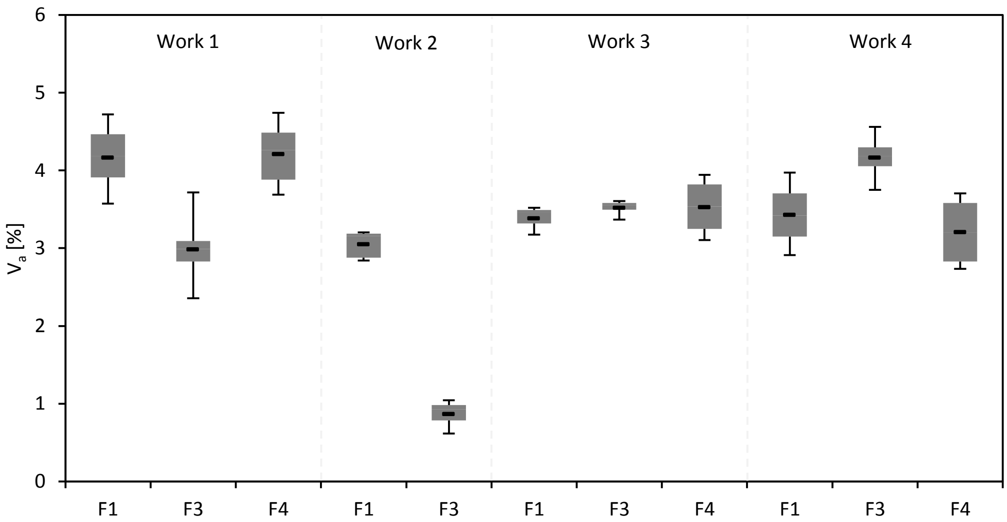

Figure 31. Individual Air void contents per work and phase

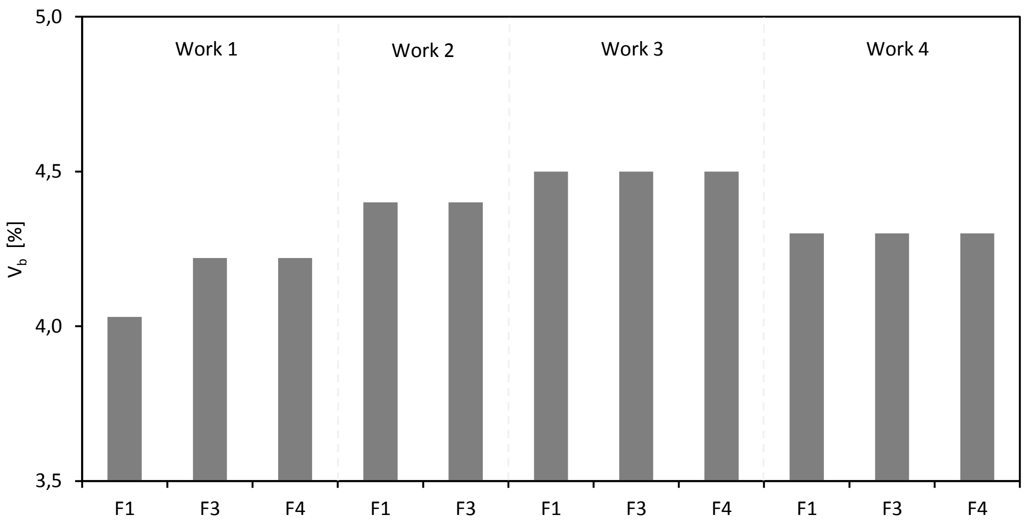

Figure 32. Individual bitumen contents per work and phase

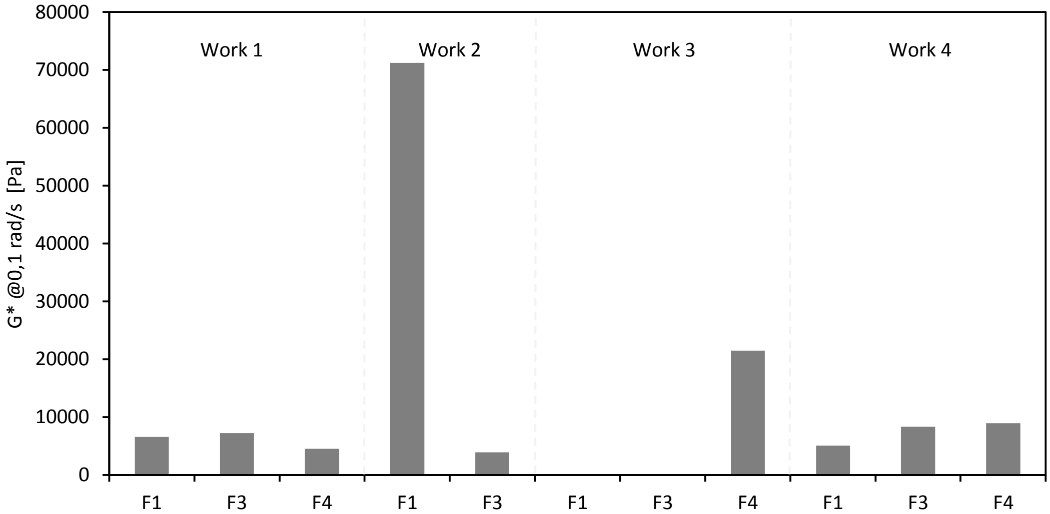

Figure 33. Individual bitumen stiffnesses per work and phase

- Density

  The majority of the density values lie above the target density, some in the acceptable +30 kg/m^3 region and some over it, meaning that the mixtures tend to be moderately to highly overcompacted. The trend of work 1 densities follows the trend of its permanent strain, with higher density leading to a higher strain level. Looking at the f_c values though, there does not seem to be a relation between them. In work 2 the image is clear that extreme compaction in the field led to excessively high rutting levels, along with high rutting rates. Work 3 shows a negative relation between density and strain levels, with small decreases in density resulting in big increases in strain levels, meaning that other factors lie behind the differences from F1 to F3 and F4. Looking at work 4, there seems to be a relation between density, ε_{1000}, and f_c, since the field specimens which are slightly more compacted, show higher strain levels and rates.

- Air void content

  Similar conclusions to those drawn regarding the density effect on the differences between lab and field can be made here. This of course was the expected case due the direct interrelation between density and air void content.

- Bitumen content

  This property was mostly studied for the comparison between the works and not between the phases, since each work has certain mixture design characteristics. The only inconsistence of this fact is in Work 1, where 0,2% less bitumen was used in F1. This could possibly explain the increased f_c values in combination with low strain levels of this phase, since less bitumen usually leads to better rutting resistance (table 9).

- Bitumen stiffness

  The most notable remark here is the extremely higher bitumen stiffness of Work 2, phase 1, not only comparing to its third phase, but also in an overall scale. The extreme deviation between F1 and F3 in work 2 seems to be coming from the extreme differences in density and bitumen stiffness. Another remarkable observation is in work, F1 and F4. Despite the bitumen ageing, bitumen's stiffness in the aged specimen is considerably lower. Surprisingly however, strain level is not affected by this fact.

The general outcome of the comparison, as described in 3.3.1, was that lab manufactured specimen give a rather optimistic indication of a mixture's performance regarding rutting. This lies mainly to the inaccuracy between the designed and the constructed characteristics, and the difficulty in achieving them precisely.

What is more, trying to trace specific observations back in the data proved to be a difficult process, not only because of certain inconsistencies, but also because permanent deformation is a multi-dimensional phenomenon. Different combinations of various factors can lead to a completely different performance, a fact which makes its prediction even more difficult. Writing down in a table the properties and parameters described before, all of them in relative comparison to the average, can demonstrate this complexity.

Table 13. Relative comparison of properties

Work	Phase	ε_{1000}	f_c	V_a	Density	VFA	Pen	G*	V_b
1	F1	Average	High	High	Average	Low	Average	Average	Low
	F3	Average	High	Average	High	Average	Average	Average	Average
	F4	Average	Very Low	High	Average	Low	Average	Very Low	Average
2	F1	Very Low	Average	Average	Average	Average	Very Low	Very High	Average
	F3	Very High	Very High	Very Low	Very High	Very High	Very High	Very Low	Average
3	F1	High	Average	Average	Average	Average	Average	-	High
	F3	Very High	Average	Average	Average	Average	Very Low	-	High
	F4	Very High	Average	Average	Average	Average	Low	Very High	-
4	F1	Average	Very Low	Average	Average	Average	Average	Very Low	Average
	F3	High	Low	High	Average	Low	Very Low	Average	Average
	F4	High	Average	Average	Average	Average	Low	Average	-

It is clear that no certain conclusion can be obtained from this table. A big number of possible combinations leads to different and many times contradictory results. One thing that can be observed with quite a certainty though, is that high accuracy in field constructed mixtures is very difficult to be achieved. The direct consequence of this is that permanent deformation performance is very sensitive and prone to change, even with minor deviations.

4. CONCLUSION

4.1 Research Conclusion

4.1.1 Water sensitivity prediction

As it was discussed, the prediction relation aiming at determining the water sensitivity of a given mixture was at a relatively acceptable levels of accuracy and reliability. Despite the fact that R^2=0,71 for ITSR, the equality line scatterplot gives the impression of a fairly good fit. The parameter multipliers suggested for predicting the water sensitivity of a mixture are the following.

Table 14. Suggested parameter multipliers for the ITSR prediction

	$ITS_{calc,dry}$	$ITS_{calc,wet}$
Intercept	-17,8580	-64,0318
V_a	-0,3614	-0,1621
VFA	-0,0531	-0,0562
Pen	-0,0147	-0,0798
logA	-8,8842	-13,9487
Density	3,4139	20,5334
G*	-0,0141	-0,0349
V_{bit}	1,4330	1,2980

Multiplying these constants with the corresponding parameters and adding them, eventually gives us the dry and wet Indirect Strength of a given mixture. Then the water sensitivity of that mixture is:

$$ITSR_{calculated} = 100 \times \frac{ITS_{calculated,wet}}{ITS_{calculated,dry}} \quad [\%]$$

4.1.2 Water sensitivity lab and field comparison

Lab specimens (phase 1) clearly showed both lower strength values and lower strength ratio values comparing to field specimens. Their performance in terms of water damage then is considered worse. In specific, specimens produced in work 3 by Van der Lee exhibit the higher resistance to water damage, both in lab and in field. The rest of the works have a poorer relation between lab and field.

One possible reason behind this inconsistency is the higher densities achieved in the field. The general trend shows a tendency for over-compacting field specimens. The result of this is less voids, thus less penetrating water in the mixture's body. The outcome of these deviations works on the safety side. Lab determination of water damage resistance is more conservative and is like having a safety factor applied. Coming to answer the fourth of the research questions stated at the beginning of the project "How well do the functional characteristics relate to field performance?", we can answer positively with respect to water damage.

However, other things need also to be considered more globally. This positive effect is the result of a mismatch with negative consequences on other performance criteria. For this reason looking at the broader image, we cannot conclude that lab and field comparison is eventually within legitimate limits.

4.1.3 Permanent deformation prediction

The outcome of the analysis in this case is different from the water sensitivity case. The prediction accuracies were not at satisfactory levels for both methods studied. With R^2=0,51 and R^2=0,57 for method 1 and 2 respectively, the prediction cannot safely be considered accurate enough. Even though the experience in the analysis at this point was still not very high because it was studied at the early stages of the internship, the observation is still that the problem does not lie on the analysis itself, but in the nature of the property and the dataset.

It is a known fact that rutting is a very complex phenomenon with a lot of parameters playing a role in its occurrence. Trying to model as many of them as possible in a predictive relation, expectedly leads to difficulties.

Another factor that affected the results is the possible inappropriateness of the MEPDG as a basis for the prediction. The formulas suggested were referring to totally different test principles and conditions. The transformations done in order to correspond them, probably led to some loss in accuracy. For this reason a safe conclusion cannot be drawn and further research following different approaches is suggested to achieve this.

4.1.4 Permanent deformation lab and field comparison

The general image is that both in terms of ε_{1000} and in terms of f_c there is a significant difference between lab and field. Lab specimen seem to perform better in rutting than the field specimen, both unaged and aged. An oddity is observed when comparing aged and unaged filed specimen with respect to ε_{1000}. They show similar values with a small tendency of aged values to be above the unaged. This is against the expectations stemming from the assumption that ageing hardens bitumen, and in consequence leads to better rutting performance.

In this case the relation of lab to field properties is characterized as optimistic. Contrary to water damage, it does not lie on the safety side and could not be used as a reliable indicator of a mixture's performance. In addition, a direct relation between the two criteria (f_c and ε_{1000}) is not observed meaning that even having a good indication for one of them, it does not necessarily lead to deducting information about the other.

This reasoning behind these changes was also more complex comparing to its counterpart on water sensitivity. In this case this reasoning was not possible just by employing the density boxplots, because no consistent trend was possible to trace. By looking at a more diverse combinations of properties some more observations could be made, but still no strong enough to support a clear conclusion. The complexity mentioned in the prediction chapter is relevant here too.

All in all, the main question of this research chapter was not to trace the differences, but to identify if there are any. This was answered quite accurately and can used as a fact.

4.2 Recommendations for further research

With the extension of NL-LAB project in 2017 and with Work 5 being added in the project's dataset, some recommendations can have a direct application and be of use.

- The new specimen that will be added will be subjected to all 4 tests used in NL-LAB. Regarding the water sensitivity determination, so far one method of conditioning the specimen was followed, the one described in the European Standard. Sometimes the information obtained from the test are insufficiently distinctive, meaning that they are not able to distinguish in detail different mixtures behaviour. For this reason different conditioning methods is suggested to also be investigated and conclude whether the result is more representative and informative. In particular two methods are proposed:

1) The moisture conditioning protocol followed in the frost damage method described in NEN 2872.
2) MIST method (Moisture Induced Sensitivity Tester) that has been proven to be able to distinguish among mixtures with different moisture damage characteristics.

In this way a broader and more detailed data set will be obtained regarding the moisture susceptibility of the mixtures tested.

- The addition of extra data can be used to further support or reject the conclusions drawn in the comparison between lab and field determined properties, and also possibly enhance the quality of the prediction relations.

- So far the triaxial tests for the determination of rutting resistance were all carried out at the same temperature and same loading conditions. Temperature is one of the most crucial factors affecting the performance of a mixture. In this way, with no variability in the tests, differences in the performance cannot be linked to the temperature's effect. It is suggested for this reason to follow a more diverse test temperature selection, that still lie within the test standards, and also assess the effect of different loading conditions.

- As it was mentioned in the conclusions, the use of the MEPDG relations as a basis is possibly a drawback for the final prediction quality. It would be more understandable and easily processed to start from point zero. Setting an initial regression equation directly for f_c and ε_{1000} and not through the logarithm of the creep compliance factor ($logD_1$) which is nowhere used in the European Standard, would certainly enhance the quality. This directness will make the analysis and its final product more friendly to the researcher and the user respectively.

- Even if the previous recommendation is not followed, the regression analysis regarding permanent deformation can be continue further in more depth. The possible parameter combinations were not studied to their maximum extent because of the aforementioned lack of experience in the early stages. For this reason, more combinations can be tested in order to possibly enhance the quality or even come to the same conclusion, that the problem indeed lies in the dataset. What is more, since all the necessary parameters are now available for both methods described in the standard (A_1, B_1, A, B, f_c and ε_{1000}) for all works, no assumptions and compromises need to be made. A more complete analysis can be made, with a direct connection to the standards.

5. REFERENCES

[1] S. Erkens, "Relating lab properties of high percentage RAP mixtures to field performance - The NL-LAB program," in *TRB*, Washington, 2015.

[2] J. Molenaar, Performance related characterization of the mechanical behaviour of asphalt mixtures, Delft, 2003.

[3] "Pavement Interactive," 22 Apri 2011. [Online].

Available: http://www.pavementinteractive.org/article/moisture-susceptibility/. [Accessed 18 November 2016].

[4] T. R. and A.-S. S., "Water sensitivity of Asphalt-aggregate mixes: Test selection," SHRP, Washington, DC, 1994.

[5] FHWA, Distress identification manual for the long-term pavement performance program, Fourth Revised Edition FHWA-RD-03-031, Washington, 2003.

[6] R. Carvalho, Prediction of permanent deformation in asphalt concrete, Maryland, 2012.

[7] "Pavement Interactive," 2008. [Online].

Available: http://www.pavementinteractive.org/article/rutting. [Accessed November 2016].

[8] McGennis, Anderseon, Kennedy and Solaimanian, Introduction to Superpave asphalt mixture design, Washington, DC: Federal Highway Administration, Office of Technology Applications, 1994.

[9] M. Miljkovic, "Rutting mechanisms and advanced laboratory testing of asphalt mixtures resistance against permanent deformation," *Facta Universitatis, Series: Architecture and Civil Engineering,* vol. 9, no. 3, pp. 407-417, 2011.

[10] E. Remisova, "Resistance to permanent deformation in binder content and film thickness viewpoint," *ACEE,* January 2013.

[11] J. Sousa, J. Craus and C. Monismith, "Summary report on permanent deformation in asphalt concrete," Institute of Transportation Studies, University of California Berkeley, 1991.

[12] "NCHRP Synthesis 274: Methods to Achieve Rut-resistant Durable Pavements," Transportation Research Board, 1999.

[13] S. K. and I. R., "Correlation of superpave G*/sinδ with rutting susceptibility from laboratory mixture tests," Transportation Research Board, 1995.

[14] " NPR-CEN/TS 15325: Bitumen and bituminous binders - Determination of Zero-Shear Viscosity (ZSV) using a Shear Stress Rheometer in creep mode," 2008.

[15] P. M. and R. C., “Binder Rheology and Asphaltic Pavement Permanent Deformation; The Zero-Shear Viscosity,” in *Eurasphalt & Eurobitume Congress*, Strasbourg, 1996.

[16] A. D., L. H. Y., P. J. and M. D., “Zero Shear Viscosity of Asphalt Binders,” Transportation Research Board, 2002.

[17] D. V. J. and V. A., “Practical test methods for measuring the zero shear viscosity of bituminous binders,” *Materials and Structure,* vol. 37, no. 5, 2004.

[18] “NEN-EN 12697-25: Bituminous mixtures - Test methods - Part 25: Cyclic compression test,” 2016.

[19] Florio, Berti, Kasbergen, Villani, Scarpas, Erkens, Sangiorgi and Lantieri, “American and European Mix Design Approaches Combined,” in *Transportation Research Board*, Washington, 2014.